2020

Surface Modification of Titanium for Orthopedic and Drug Delivery Applications

Prantik Roy Chowdhury
prantik2526@gmail.com

ABSTRACT

SURFACE MODIFICATION OF TITANIUM FOR ORTHOPEDIC AND DRUG DELIVERY APPLICATIONS

Prantik Roy Chowdhury, MS
Department of Mechanical Engineering
Northern Illinois University, 2020
Dr. Sahar Vahabzadeh, Director

Titanium is one of the most attractive metals used in orthopedic and drug delivery applications because of its excellent mechanical properties, biocompatibility and high corrosion resistance. However, due to its bio-inertness, fibrous tissue forms between the bone and implant which causes loosening of the implant. Surface modification can play an important role to enhance interaction between implant and the surrounding tissues, which reduces the implant failure. The aim of this study is to a) incorporate magnesium (Mg) into modified titanium surface by different deposition methods for bone-implant interaction, b) modify the surface of titanium by alkali treatment, and c) investigate the release behavior of aloe-emodin (AE) from surface-modified titanium substrate.

Different deposition methods were used to investigate the doping of magnesium content on titanium-modified surface. Our result showed that the magnesium content on titanium-modified surface was enhanced with the increase of magnesium precursor concentration in the deposition solution. Alkali treatment was performed using different concentrations of NaOH, temperatures and rotation of speeds and we found these parameters affect formation of web-like or nearly web-like structures on polished titanium samples. Release behavior of AE from modified Ti samples

was controlled by applying PLGA coating at different PLA:PGA ratios, and increase in osteoblast cell adhesion and proliferation was found in polymer-coated samples.

In conclusion, the study investigated various routes to modify the surface of Ti for drug delivery and bone tissue engineering application.

NORTHERN ILLINOIS UNIVERSITY
DEKALB, ILLINOIS

AUGUST 2020

SURFACE MODIFICATION OF TITANIUM FOR ORTHOPEDIC AND DRUG DELIVERY APPLICATIONS

BY

PRANTIK ROY CHOWDHURY

A THESIS SUBMITTED TO THE GRADUATE SCHOOL

IN PARTIAL FULFILLMENT OF THE REQUIREMENTS

FOR THE DEGREE

MASTER OF SCIENCE

DEPARTMENT OF MECHANICAL ENGINEERING

Thesis Director:
Sahar Vahabzadeh

ACKNOWLEDGEMENTS

I would like to show my gratitude for everyone who has given support during my research work. Specially, I am very much grateful to my respected advisor, Professor Dr. Sahar Vahabzadeh, for her support and valuable advice from the very beginning of my master's program. Without her proper guidance and direction, this would have been impossible for me to complete. I have always been motivated by her attitude towards my research work. She stirred me to take right decisions while doing research work. I am also thankful to my committee members, Professor Dr. Iman Salehinia, Professor Dr. Bobby Sinko, and Professor Dr. Jifu Tan, for their valuable suggestions for my research work. I would like to thank Dr. Paige Bothwell, research scientist at NIU, for her support in biological research work. Without her support, it would have been difficult for me to finish the biological research work successfully. I am very lucky to be a member of such a nice research group. I am really thankful to Joshua Marbel, Sarah Fleck and Matthew Kleszynski for helping me during my research work. I would also like to thank Stephen Binderup, lab manager of MRDL at NIU, for his help during microscopic analysis. I would like to thank Gregg Westberg for giving me training on scanning electron microscope (SEM). I also thank Murali Krishna Duvvuru for his help from the beginning of my research. Finally, I would like to thank my parents, my beloved wife, my elder brother and my friends who give me support and encouraged me to finish the work successfully.

DEDICATION

This work is dedicated to my beloved parents, wife, family and friends who have given me continuous support, blessings and wishes to make the work possible.

TABLE OF CONTENTS

Page

Page

Page

LIST OF TABLES

Page

LIST OF FIGURES

Page

CHAPTER 1 INTRODUCTION

1.1 Metallic Implants

Metallic materials have been used as medical implants since the 19th century [1] and are being used in almost 95% of orthopedic applications [2]. Almost $41.1 billion growth in orthopedic industry was recorded in 2016 [3]. Most of the people in developed countries who are more than 50 years old have been affected by bone and joint degenerative problems and the numbers will be doubled by 2020 [4]. The goal of the metallic implant in orthopedic surgery is to relieve pain and restore function of the bone and joint [3]. In addition, durability of metallic implants is also increasing attention from the orthopedic industry [3]. The survivorship of total knee replacement and hip replacement after 15 years ranges from 81.7% to 98.14 % and over 90%, respectively [3]. In order to ensure long-term effectiveness, the metal should have desirable mechanical properties like strength, toughness and biocompatibility to the human body [2]. Figure 1 shows different applications of metal used in orthopedics. In addition, the human body is favorable to accelerate corrosion; therefore, appropriate selection of metal is of paramount importance to increase the lifetime of implanted metal [4]. The selected metal must be bio-inert to prohibit corrosion reactions and metal ion leaching [4].

There are different types of metal used as biomaterials that have different functions. Stainless steel, titanium, cobalt-chromium alloy, nitinol, among others, are used for orthopedic purposes.

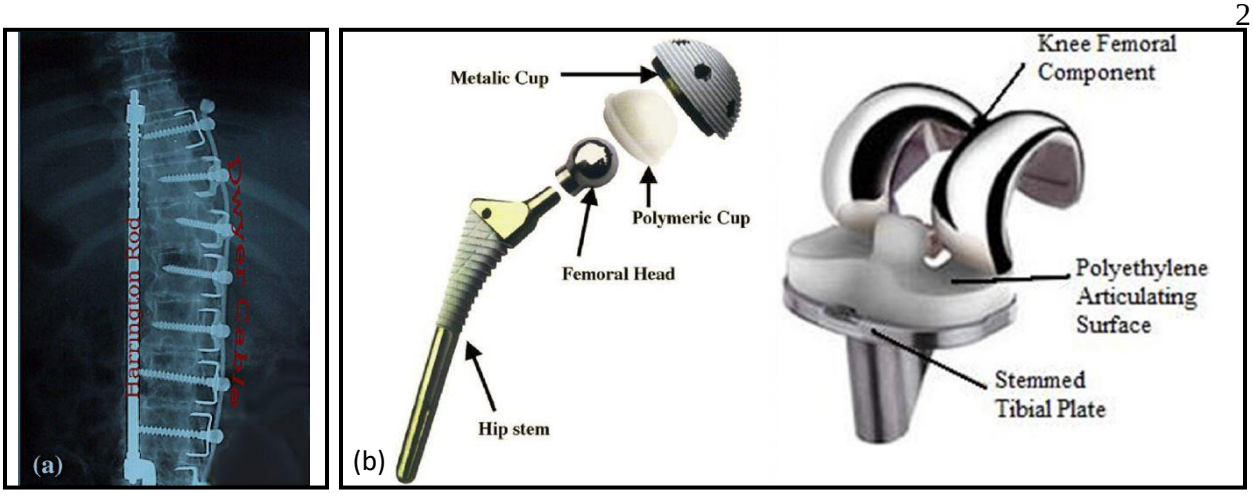

Figure 1: (a) The Harrington rod, a stainless-steel surgical device (b) Artificial hip joint (left) and knee implant (right) [1,5].

Stainless Steel:

Stainless steel has been used as a medical implant since the 1920s because of its good corrosion resistance behavior and mechanical properties [6]. There are different categories of stainless steel available commercially, but not all of them are suitable for metal implant applications because of their chemical compositions and mechanical properties [6]. In general, the stainless steel in austenitic phase is non-magnetic, which causes significant displacement and heating effects that distort its effectiveness. In addition, the stainless steel can form different phases in austenite, like the delta phase during metal processing, which has deleterious effects in human body [6]. Table 1 shows different types of stainless steel based on compositional range used as implant.

316 L stainless steel is referred to as surgical stainless steel by the American Iron and Steel Institute (AISI). The content of alloys composition is mentioned in Table 1. Due to the presence of molybdenum (3 wt%), corrosion resistance behavior increased, which prohibits intergranular attack and pitting corrosion [6, 7]. Low carbon content (<0.03 wt%) prevents formation of

chromium carbide as 17-19 wt% chromium presence in 316 L stainless steel [6,7]. In addition, due to the alteration of composition, nickel induces into the 316 L, which makes the metal stable at high temperature [6, 7].

Table 1: Composition (weight percentage) of implantable stainless-steel alloy [6]

Alloy	Cr	Ni	Mn	Mo	C	N	Nb	V	Si	Cu	P	S
316L ASTM F138, ISO 5832-1	17–19	13–15	<2 max	2.25–3	<0.030	<0.10	–	–	<0.75	<0.5	<0.025	<0.010
22-13-5 ASTM F1314	20.5–23.5	11.5–13.5	4–6	2–3	<0.030	0.2–0.4	0.1–0.3	0.1–0.3	<0.75	<0.5	<0.025	<0.010
Rex 734, Ortron 90 ASTM F1586 ISO 5832-9	19.5–22	9–11	2–4.25	2–3	<0.08	0.25–0.5	0.25–0.8	–	<0.75	<0.25	<0.25	<0.010
BioDur® 108 ASTM F 2229	19–23	<0.050	21–24	0.5–1.5	<0.08	0.85–1.10	–	–	<0.75	<0.25	<0.03	<0.010

Cobalt-Chromium Alloys (Co-Cr alloys):

Cobalt-chromium alloys have been used in orthopedic, dental and manufacturing stents because of its good mechanical properties, corrosion resistance behavior and high wear resistance properties [8,9]. This alloy has high Young's modulus (210 GPa), yield strength (448-648 MPa) and tensile strength (951-1220 MPa) [9]. The Co-Cr alloy has favorable corrosion resistance due to the presence of over 20% of chromium into the alloy, which forms a chromium oxide passive layer on the surface [8]. In addition, their wear resistance properties are also higher compared to titanium and stainless steel [8]. However, Co-Cr alloys have cytotoxicity and inflammatory response to the human body [10].

Co-Cr has different types of alloys, such as Co-Cr-Mo alloy and Co-Ni-Cr-Mo-Ti, which are also used as implants because of their mechanical strength and hardness properties [8,11]. Moreover, the use of Co-Cr alloys has become a major concern due to nickel toxicity that causes allergic reaction to the body [12].

Titanium and Its Alloy:

Titanium and its alloys are now receiving attention as metallic implant because of their high strength, low density and Young's modulus, high corrosion resistance, biocompatibility and no allergic reaction to the body compared to stainless steel and Co-Cr alloys [5,6]. Table 2 shows a comparison among tensile strength, yield strength and elastic modulus of different metallic implants with bone.

Table 2: Comparison of tensile strength, yield strength and elastic modulus of different metallic implants with bone [13]

Material	**Tensile strength (MPa)**	**Yield strength (MPa)**	**Elastic modulus (GPa)**
Bone (cortical)	70-150	30-70	15-30
Stainless Steel	490-1350	190-690	200-210
Co based alloys	655-1793	310-1586	210-253
Titanium based alloys	690-1100	585-1060	55-110

Pure titanium (cp-Ti, grade 2) and Ti-6Al-4V (grade 5) alloys are commonly used in orthopedic and dental applications because of their low elastic modulus, which causes less stress shielding effect [5]. Stress shielding effect is defined as the mismatching of Young's modulus between the bone and implant, which causes non-homogeneous stress transfer [14]. This stress transfer causes loosening of implants [14].

The main property of titanium and its alloy is the formation of an oxide layer by spontaneous passivation or re-passivation process, which makes the metal and its alloy

biocompatible and highly corrosion resistant while also making it bio-inert [5, 15, 16]. The human body isolates the implant due to its bio-inertness behavior that forms fibrous tissue, causing the loosening of the implant [17]. However, titanium and its alloy have thinner fibrous encapsulation compared to stainless steel and Co-Cr alloy [13].

The main drawbacks of titanium and its alloy are the poor fretting fatigue resistance and tribological properties due to its low hardness, which cause high coefficient of friction. This high coefficient of friction releases wear debris from implant to bloodstream, resulting in the inflammation of the surrounding tissue and the increase of the bone resorption [5]. Figure 2 shows the wear debris due to a sliding tribological coating with the presence of third bodies.

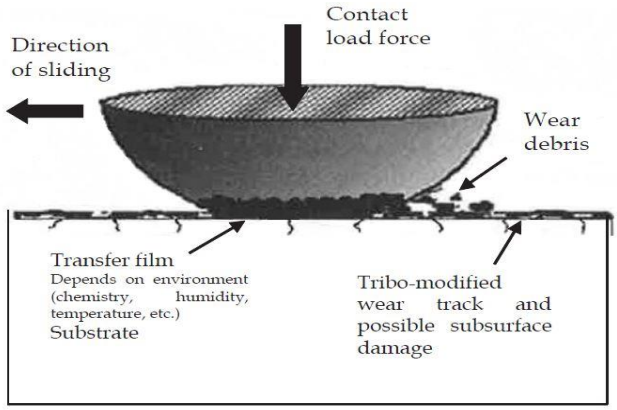

Figure 2: Reason of wear debris due to a sliding tribological coating [5].

1.2 Importance of Surface Modification

Surface modification is necessary to enhance the performance of implants by improving the tribological properties, corrosion resistance and osteointegration [5]. When material is implanted into the body, at first, blood comes in direct contact with the implant, which causes the blood protein adsorption at the solid-liquid interface [18]. These proteins have some conformational changes which increase the biological interaction between the bone and implant

[18]. The protein adsorption depends on exposure time, and strong adsorption increases biological interactions [18]. Surface modification can ensure good anchoring of the implant and surrounding tissue that increases bone conductivity and inductivity, improves biocompatibility and bioactive fixation, and enhances lifetime of the implant [19]. Table 3 shows different surface modification techniques on titanium and its alloy, as well as their objectives.

1.3 Surface Modification Methods

1.3.1 Anodization Process

Many methods have been used to obtain nanostructure on the surface of titanium and its alloy. Electrochemical anodic oxidation process is one of the suitable methods to form nanotubes on the titanium surface [18]. Figure 3 shows the set-up of electrochemical anodization process consisting of electrolyte, titanium as anode, platinum foil as cathode and power supply.

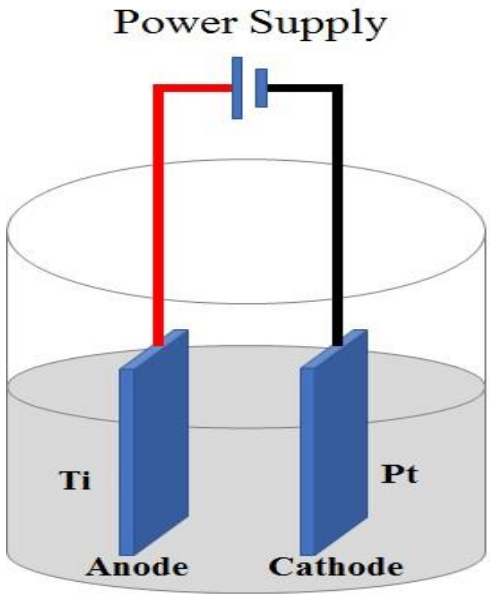

Figure 3: General set-up of electrochemical anodization process.

Table 3: Surface modification techniques on titanium and its alloy, and their objectives [19,20]

Surface Modification Methods	**Objectives**
Mechanical Methods • Machining • Grinding • Polishing • Blasting	• Produce expected surface topography and improve adhesion in bonding.
Chemical Treatment • Alkali treatment • Acidic treatment • Hydrogen peroxide treatment • Sol- gel • Anodic oxidation • Chemical vapor deposition (CVD) • Biochemical methods	• Improve biocompatibility, bioactivity and bone conductivity. • Increase corrosion resistance and wear resistance properties and blood compatibility. • Removal of contamination.
Physical Methods • Thermal spray: flame spray, plasma spray, high velocity oxygen fuel (HVOF), detonation gun spraying (DGUN). • Physical vapor deposition (PVD): Evaporation, Ion plating, sputtering • Ion implantation • Glow discharge plasma treatment	• Improve wear resistance, corrosion resistance, blood compatibility and bioactivity.

The purpose of the electrochemical anodic oxidation process is to form TiO_2 nanotubes on the surface. The growth of the TiO_2 follows three steps: electrochemical oxidation of Ti into TiO_2, electric-field-assisted dissolution titanium into the electrolyte solution, and fluoride ion dissolution and balance of growth [21, 22]. The formation of TiO_2 can be expressed by the following chemical reactions [21]:

$$Ti \rightarrow Ti^{4+} + 4e^{-} \quad (1)$$

$$Ti^{4+} + 2H_2O \rightarrow TiO_2 + 4H^{+} \quad (2)$$

$$TiO_2 + 4H^{+} + 6F^{-} \rightarrow TiF_6^{2-} + 2H_2O + 2H^{+} \quad (3)$$

During the anodization process, titanium is immersed into the electrolyte as an anode that forms an oxide layer on the surface. The pitting and decomposition occur in the oxide layer due to the presence of fluoride ion into the electrolyte resulting in the formation of uniform nanotube structure throughout the surface. The schematic diagram of TiO_2 nanotube formation is shown in Figure 4.

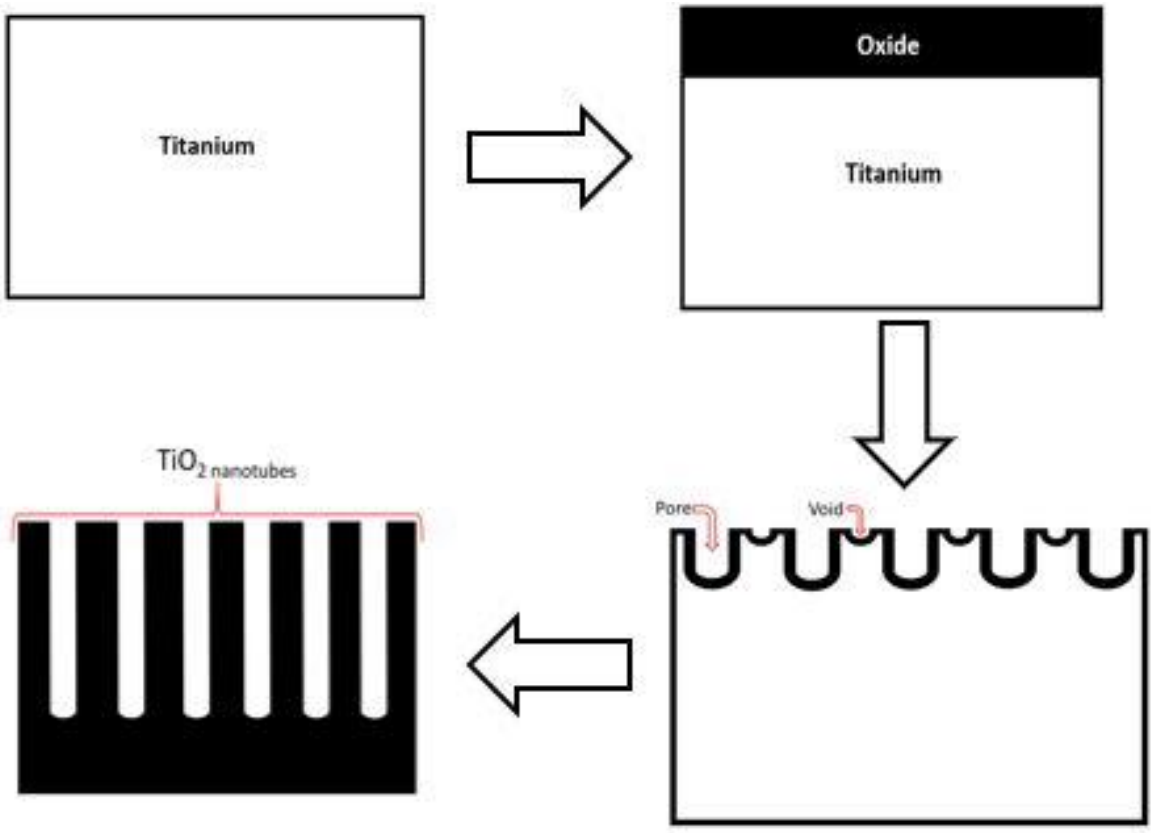

Figure 4: Schematic diagram of TiO_2 nanotube formation.

The nanotube formation by anodic oxidation process depends on different parameters like electrolyte, applied voltage, anodization period, pH of the electrolyte, and temperature [23]. The oxide growth, uniform TiO_2 formation, precipitate and non-uniform oxide formation, and gap formation between nanotubes depend on the electrolytes used for anodization [23]. There are different types of electrolytes used in the anodization process, like HF, NH_4F, CH_3COOH, H_2SO_4, Na_2HPO_4, NaF, Na_2SO_4 NaOH, NH_4Cl, CSF, and KF [23]. Applied potential is another important factor to control the diameter of the nanotube [22]. Lowering the voltage implies lowering the diameter of the nanotubes [22]. Low voltage forms a compact TiO_2 layer; while high voltage causes a sponge-like porous structure [22]. In addition, anodization period influences the length of nanotubes [23], and optimum anodization temperature (20-40 °C) does not have any impact on the nanopore structures [24]. However, when temperature is higher or equal to 50°C, nanostructures are not observed due to the faster chemical etching rates compared to oxide formation reactions [24].

Anodization is a promising method to enhance the biological properties of the titanium in orthopedic and drug delivery systems [22,25]. The nanostructure of the titanium has altered physical and chemical properties to enhance osteoblast adhesion, proliferation and long-term cellular functions [25]. Nano-phase structure increases fibronectin and vitronectin adsorption 15% and 18% respectively compared to conventional titanium [26].

TiO_2 nanotubes are biocompatible because of their antibacterial properties, low cytotoxicity, enhanced adhesion, proliferation, osteointegration and differentiation properties in orthopedics [22]. The nanotube diameter also has an effect on osteoblast interaction. If the nanotube diameter is less than 15 nm, osteoblast adhesion and differentiation increase [27,28]. If

the diameter is more than 50 nm, cell activity decreases [27,28]. However, when the diameter is between 60 to 80 nm, no significant difference in cell activity is observed in between the polished surface and the nanotube surface [28,29]. A nanotube diameter greater than 80 nm shows significant bone-bonding strength compared to grit-blasted titanium [28, 30]. A large nanotube diameter (100 nm) ensures increased osteoblast elongation [31]. So, increase in nanotube diameter enhances elongation or stretch of cell bodies, which improves bone forming ability [31].

1.3.2 Alkali and Heat-Treated Treatment

Alkali and heat treatments (AHT) are two most simple and economical processes of forming porous network structure on the surface of titanium [32]. The main advantage of alkali treatment is to form uniform porous network structure on the surface that shows direct bonding to the bone, improved attachment and bone ingrowth into the porous network structure [32]. Alkali treatment forms hydrated titanium oxide gel ($HTiO_3^+$) on the surface, which contains alkali ions [33]. After heat treatment, alkali-titanate layer has been formed into the surface, and alkali ions are released from titanate layer when exposed to body fluids, resulting in the formation of titanium-oxide layer containing calcium and phosphate ions [33]. Figure 5 represents the structure change of pure titanium due to alkali treatment and heat treatment and the mechanism of alkali heat-treated sample in SBF solution [34].

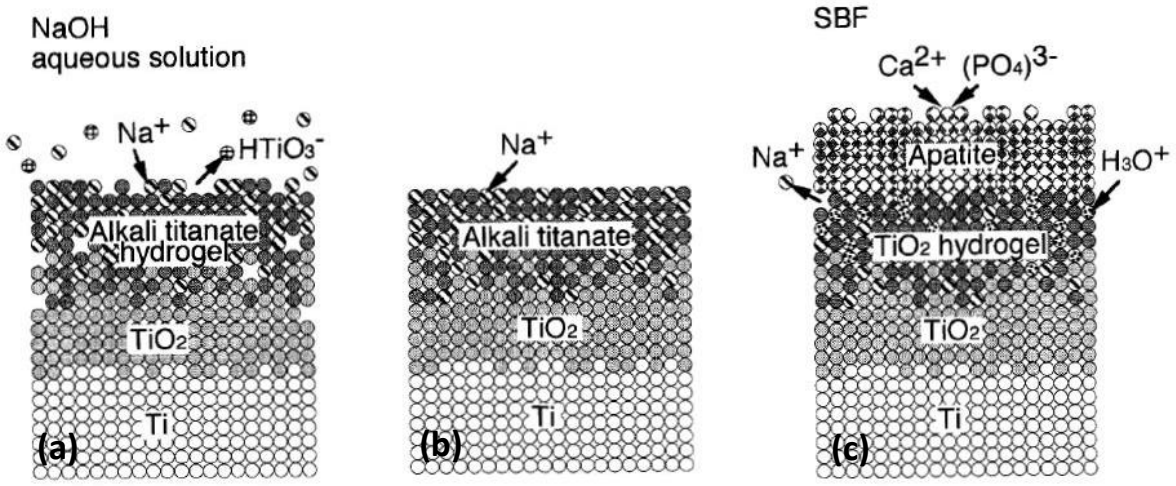

Figure 5: (a) Formation of alkali-titanate hydrogel by alkali treatment (b) Densification of hydrogel in titanate due to heat treatment (c) Apatite formation in SBF [34].

The combined effects of alkali treatment and heat treatment ensure optimal condition of bone marrow cell adhesion and bone differentiation [35].

1.3.3 Ion Incorporation

There are different types of techniques used for ion incorporation into the titanium metal, such as the anodization process, immersion method and physical vapor deposition (PVD).

Immersion Method:

Immersion method is one of the techniques to incorporate ions into the titanium. In this method, the surface is modified by using different surface modification techniques like anodization or alkali treatment. After surface modification, titanium is immersed into the immersion solution, prepared by precursor of the expected ion, for a certain period to ensure bonding of the ion into the titanium lattice [36]. The schematic diagram of the immersion methods for ion incorporation is shown in Figure 6.

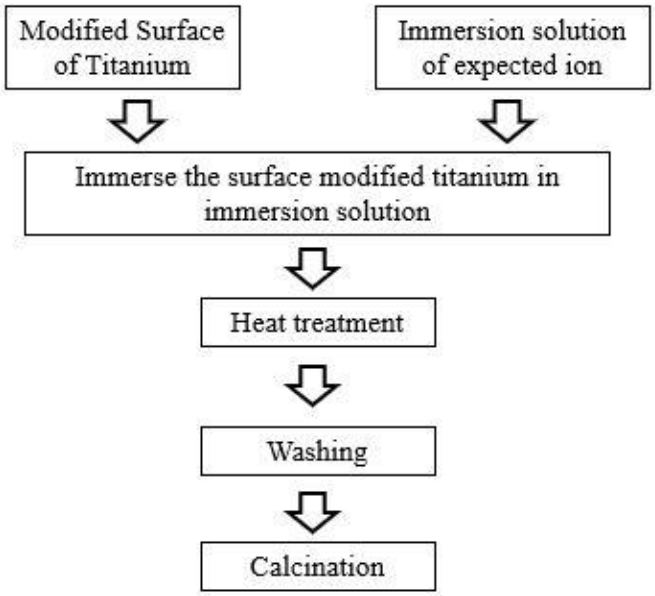

Figure 6: Schematic diagram of the immersion method [36].

Physical Vapor Deposition (PVD):

Physical vapor deposition (PVD) is a widely used technique in the metal working industry, biomedical applications and manufacturing electrical components by applying coating with enhanced properties like low friction, high hardness, high wear and corrosion resistance properties, etc. [37]. It is a vacuum deposition process where material goes from condensed phase to vapor phase and then back to a thin-film condensed phase to apply a thin film or coating [38]. The most common two types of PVD are sputtering and evaporation [38].

Sputtering Process:

During the sputtering process (Figure 7), atoms in the nearest surface have got momentum and sufficient energy by impact to overcome binding energy to emit from the surface [39]. The most common types of sputtering processes are ion beam sputtering and magnetron sputtering [40]. In ion beam sputtering, an ion source is being used to generate ion beams that are directed to

the target [40]. In magnetron sputtering system, positively charged ions from plasma are accelerated by an electric field imposed to the negatively charged target [40].

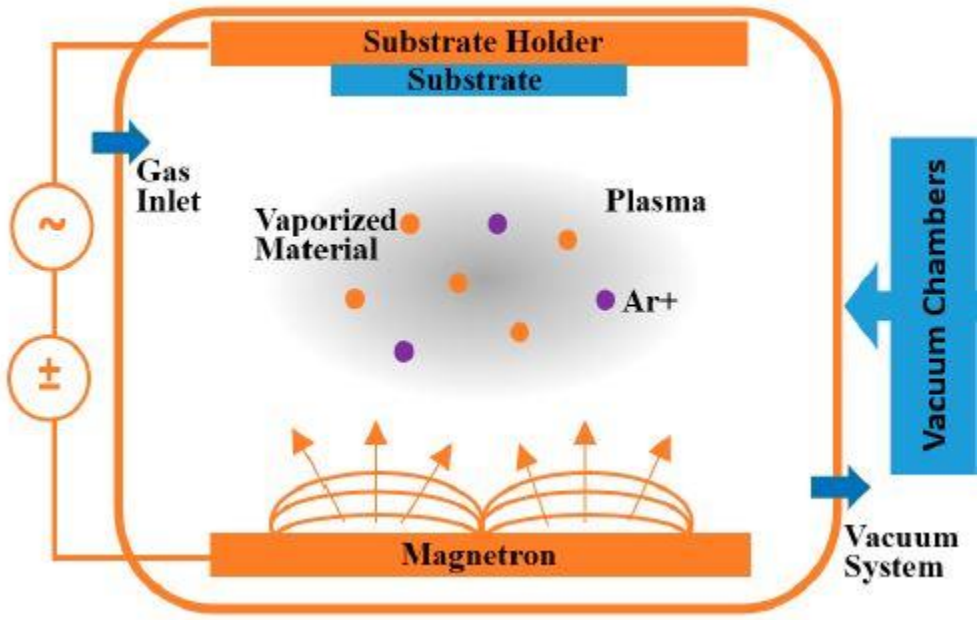

Figure 7: Schematic drawing of sputtering process [41].

Electron Beam Deposition (E-Beam PVD):

E-beam evaporation (Figure 8) is a physical process where the target acts as an evaporation source and is bombarded by electron beams at high vacuum pressure, causing atoms of the source material to evaporate into the gaseous phase [41]. These atoms then precipitate in solid form and finally form a coating layer of vacuum chamber [41].

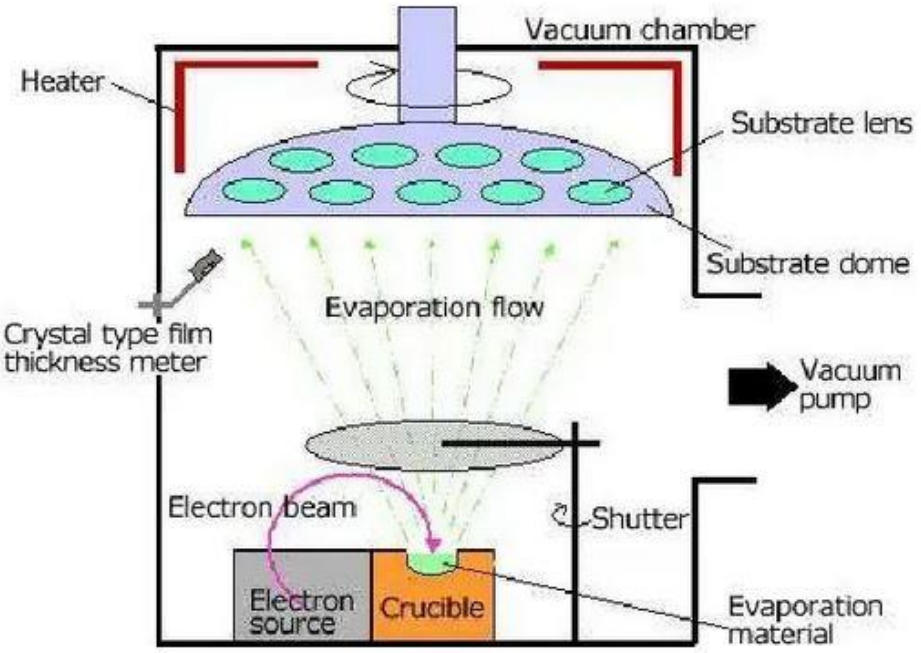

Figure 8: Schematic diagram of electron beam deposition (e-beam) process [41].

1.4 Role of Incorporated Element

Most of the materials are not completely inert in the human body, so selection of the materials is based on the elements already existing in the body [1]. Some of the elements are present in the bone as minerals or in blood as Ca, P, Mg, while some of the elements exist as electrolytes in the extracellular fluid [1]. Small amounts of elements present in the body may have significant effects on the human body [42]. Those trace elements act as co-factor of the enzymes and stabilize the structure of the protein [42]. However, the concentration of those elements at higher levels causes toxicity to the human body [1,42]. Table 4 shows different types of trace elements found in the human body.

Table 4: Elements and their compositions in the human body [1]

Element	O	C	H	N	Ca	P	K	S	Na	Cl	Mg	Trace element
Wt%	65	18.5	9.5	3.3	1.5	1.0	0.4	0.3	0.2	0.2	0.1	<0.01
At%	25.5	9.5	63.0	1.4	0.31	0.22	0.06	0.05	0.3	0.03	0.1	<0.01

Although the role of the trace elements is somewhat unclear, those trace elements play an important role for bone synthesis [43]. The lack of trace elements in the body causes osteoporosis [43].

Iron:

Iron is one of the essential elements in the body and involves the synthesis control of bone matrix [42,44]. The total iron content in the human body is around 3-5 g, 75% of which remains in the blood [42]. The rest of the iron is present in the bone marrow, liver and muscles [42]. The lack of iron causes anemia, poorly mineralized skeletons and pathological change in microarchitecture of trabecular bone, whereas excessive iron in the body can enlarge the liver and can be responsible for heart failure [1,44].

Magnesium:

Magnesium is the fourth most abundant element in the human body [45]. The total content of magnesium in newly born babies and adults is around 0.8 g and 25 g respectively; 60% of magnesium exists in the bone [45]. The presence of magnesium ions enhances osteoblast cell adhesion and proliferation, which accelerates new bone formation [46-48]. It also plays an important role for bone metabolism [46].

Calcium:

Calcium is one of the most abundant elements present in the human body [45]. The total content of calcium in newly born babies is around 28 g [45]. Almost 99% of the total calcium exists in the skeleton and only a small amount of calcium is present in the plasma and extravascular fluid [45]. It plays an important role in the formation of new bones and enhances osseointegration in the early postoperative period [49].

Strontium:

Strontium is another trace element that enhances bone formation and reduces resorption by decreasing osteoclast differentiation [50,51]. Strontium at low concentration does not have any deleterious effect on bone matrix mineralization [51,52].

Silver:

Silver is used in orthopedic applications because of its antimicrobial properties [53-55]. However, silver ion may have toxic effects due to metal ion leaching [53]. The presence of silver ions in a metallic implant like titanium enhances bone formation and osseointegration [56]. Controlled release of silver nanoparticles from the implant can ensure biocompatibility [55].

Zinc:

Zinc is another essential element in the human body. The average zinc content in adults is around 2-3 g and 99% of this is present in the intracellular matrix; the rest is found in the plasma [42]. Zinc is necessary for reproductive function because of its role in follicle-stimulating hormone (FSH) [1]. Zinc enhances bone formation and accelerates synthesis of collagen [44].

Manganese:

Manganese is also an important trace element in the human body. The total manganese content of an adult human body is around 15 mg [42]. Bone, liver, kidney and pancreas have higher manganese concentrations than other tissues [42]. Manganese deficiency disrupts bone formation [1, 44] and leads to reproductive disorders [1].

Copper:

Copper is a co-factor of antioxidant enzymes which removes the free radical caused by the activation of osteoclast [44]. In addition, it directly inhibits the osteoclast resorption and maintains the optimal state of the bone matrix [44]. The copper content has significant impact on bone health. Lower serum copper level decreases body mineral density (BMD) of femur and femoral neck, while higher serum copper level causes fracture of the bone [57]. Moderate serum level ensures favorable bone health [57].

Boron:

Boron is a micro-nutrient which is essential for bone mineral metabolism and inhibits osteoporosis [58]. It enhances bone growth and maintenance of the bone [44]. It also increases the bone stiffness, and lack of boron in the human body may cause defect of skeleton development [44].

1.5 Purpose of Drug Delivery

Drug delivery is a process of dispensing pharmaceutical compounds to obtain therapeutic effect in the human body [59]. It has been advanced for the last six decades with a large number of formulations introduced in clinical applications [60]. Oral drug dosing is not always effective

due to the damage of non-targeted cells in some parts of the body [61]. In addition, oral drug dosing and other injectable depot formulations presents some difficulties due to the hydrophilic nature and high molecular weight of drugs [60]. Moreover, the duration of drug release and drug delivery to the targeted cells are also a major concern to get the desire properties of the implanted area [60]. So, controlled delivery, slow delivery and targeted delivery are attractive methods of using drug delivery in the human body to get the desired output into the infected area [60].

The purpose of the drug release dynamics is to understand the process of release and its dynamic characteristics, which depends on the polymer coating, drug properties like hydrophobicity or hydrophilicity, dose, dose form and effect of drug [62].

Skeletal diseases and prevention of postsurgical diseases are challenging because of the complex and solid structure of bone which limit the blood supply and therapeutics diffusion [63]. Titanium and its alloy with modified surface can solve this problem by improving osseointegration, reducing inflammation and infection by facilitating localized drug delivery (LDD) to cure bone disease as well as cancer [63]. Titanium nanotubes (TNT) structure is suitable for localized drug delivery although the drug release from TNT is quick [64]. pH and polymer coating can control the release of drug from TNT [64, 65]. Different types of polymer can be used to coat the drug-loaded TNT like gelatin, chitosan, polycaprolactone, poly(lactic acid) and poly(lactic-co-glycolic acid) (PLGA). A study on drug delivery from TNT coated with polymer and effect of pH on drug release reported that TNT coated with PLGA improved the drug release profile [65]. Figure 9 shows the drug release into the buffer medium by polymer swelling during the critical time t_1 and drug released completely due to polymer degradation into the time period of t_2 [64].

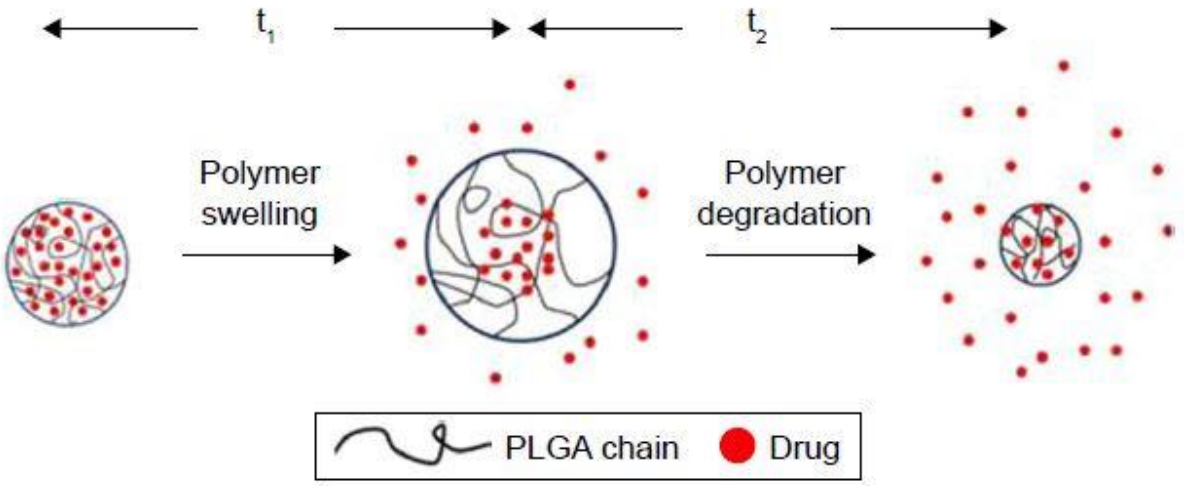

Figure 9: Schematic diagram of pH-dependent drug release from polymer [64].

1.6 Research Objectives

This research is focused on magnesium incorporation into titanium nanotubes by immersion method, single-step anodization technique and reverse polarization method to obtain optimum doping of magnesium into the nanotubes. The research is also focused on surface modification of titanium by anodization forming nanotube structure to investigate drug release profile and effect of controlling drug release from the nanotubes in orthopedic applications. Alkali treatment at different temperatures and rotational speeds is also investigated to form uniform web-like or nearly web-like surface structures and their effectiveness on *in vitro* biological properties.

Objective 1: Magnesium-Deposited Surface-Modified Titanium for Orthopedic Applications.

Incorporation of magnesium into the titanium nanotubes was carried out by immersion methods, single-step anodization and reverse polarization methods to get optimum surface morphology followed by magnesium deposition into the nanotubes.

Objective 2: Controlled Release of Aloe-Emodin from Surface-Modified Titanium and Its *in Vitro* Interaction with Human Osteoblast Cells.

Anodization method was carried out to form uniform nanotube structure on the surface and aloe-emodin was loaded into the nanotubes followed by PLGA coating. After that, controlled release of aloe-emodin from nanotube surface was investigated and *in vitro* interaction of aloe-emodin with human osteoblast cells was also studied.

Objective 3: Surface Modification of Titanium by Alkali Treatment for Orthopedic Application.

Alkali treatment at different rotational speeds and temperatures was carried out to form web-like or nearly web-like structures.

CHAPTER 2 COMPARATIVE STUDY FOR SUCCESSFUL DEPOSITION OF MAGNESIUM ON SURFACE-MODIFIED TITANIUM FOR BIOMEDICAL APPLICATIONS

2.1 Introduction

Titanium and titanium alloy-based implants are an inevitable part of orthopedic and dental applications due to their biocompatibility, corrosion resistance, fatigue resistance and high elastic modulus [66-67]**.** The corrosion resistance behavior is due to the native oxide layer which is formed by the exposure of titanium to the air at room temperature [15,68]. This native oxide layer also makes the implant surface bio-inert [20]. The bio-inertness behavior is responsible for the formation of fibrous tissue and the lack of osseointegration, resulting in the loosening of the implant [15,69]. In order to increase osseointegration and durability, the surface of the titanium implant needs to be modified by different surface modification methods like plasma spraying [70, 71], anodization [72, 73], alkali treatment [32-35], sol gel [74, 75] and so on. Anodization is one of the surface modification techniques used to form nanotubular structures on the implant surface that enhance cell adhesion, proliferation and differentiation [76]. The main advantages of TiO_2 nanotubes are uniform structure on the surface, high specific surface area, favorable mechanical and chemical stability, and charge transport property [77, 78]. In addition, incorporation of various bioactive molecules or ions into the nanotubular structure enhances bioactivity of the implant [79].

Incorporation of bioactive trace elements like strontium, magnesium, iron, and calcium is now gaining attention in orthopedic application due to their stability, flexible storage environment and suitable fabrication methods that facilitate apatite forming ability, bone growth and bone healing by enhancing osteoblast activity [46, 72, 80-82]. The elements can be deposited into the titanium by different methods: electrochemical anodic oxidation process [83, 84], sol-gel route [85], photo-assisted deposition method [86], ultrasound-assisted impregnation-calcination method [87], and reverse polarization [88].

Magnesium is one of the essential trace elements in the human body. The total content of magnesium in a newly born baby and an adult is around 0.8 g and 25 g respectively, 60% of which exists in the bone [45]. Magnesium is important for bone metabolism and to stimulate bone formation because concentration of incorporated magnesium accelerates osteoblast cell proliferation [46, 72, 89, 90]. In addition, magnesium prevents osteoporosis, which happens due to decrease of new bone formation and increase of bone resorption of the human body [72]. Many studies have been performed to incorporate magnesium into the modified titanium surface. Wang et.al. [46] performed a study on magnesium ion incorporation into titanium nanostructure where hydrothermally fabricated TiO_2 nanostructure was used to deposit magnesium ions at different concentrations using plasma-immersion ion implantation process. Other research was performed to study magnesium ion deposition into TiO_2 nanotubes to enhance osteogenic differentiation of bone marrow mesenchymal stem cells (BMSCs) [72]. In the research, magnesium-doped titanium nanotube was fabricated using electrochemical anodization and ion exchange method where magnesium content in titanium nanotube increased with increase of magnesium acetate concentration in the solution [72].

The aim of this study is to use different techniques to incorporate magnesium in titanium-modified surface. The hypothesis of this study is validated by the fabrication of modified titanium surface with different concentrations of incorporated magnesium ions. To accomplish the aim, surface morphology and magnesium content were investigated by field emission scanning electron microscope (FESEM) and energy-dispersive X-ray spectroscopy (EDS).

2.2 Materials and Methods

2.2.1 Materials

Commercially pure titanium (cp-Ti grade #2, President Titanium, MA, USA), ethanol (200 proof anhydrous), acetone (certified ACS), hydrofluoric acid (48-51% solution in water), and magnesium nitrate hexahydrate ($Mg(NO_3)_2 \cdot 6H_2O$, BioXtra, ≥98%, obtained from Sigma Aldrich USA).

2.2.2 Methods

In this work, three different methods of immersion, single-step anodization, and reverse polarization were used to investigate the effective parameters of successful preparation of Mg-deposited nanotubular structure on Ti. Prior to each method, commercially pure titanium disks with a diameter of 11 mm and a thickness of 2 mm were ground by silicon abrasive paper (grits 320, 400, 600 and 800), followed by polishing. Samples were then washed and cleaned by nano-pure water, ethanol, acetone and finally dried it at ambient temperature.

Immersion Method:

In immersion method, anodization was performed using 1 vol. % HF electrolyte at 20V for 45 minutes, as explained in detail in our previously published work [91]. Briefly, anodization was

carried out in 1 vol. % HF electrolyte solution at 20 V for 45 minutes; titanium disk and platinum foil (Alfa Aesar) were used as anode and cathode respectively. After anodization, titanium substrate was rinsed with DI water and dried at atmosphere.

Anodized samples with nanotubular surface structure were then used to deposit Mg using immersion method. Immersion solution prepared by magnesium nitrate hexahydrate was stirred at 35°C for 0.5 h. Samples were immersed in magnesium nitrate hexahydrate solution in nano-pure water for 24 h. Samples were then removed from the solution and dried in oven at 60°C for 2 h. To understand the role of the solution concentrations, sequence of calcination and cleaning processes, two different routes were used as subsequent stages after drying. In the first route, 0.6 g magnesium nitrate hexahydrate in 50 ml nano-pure water was used. After subsequent drying, samples were washed with nano-pure water and then calcined at 300 °C for 2 h with a rate of 10°C/ min [36]. In the second route, three different concentrations of 0.6 g, 1.0g and 2.0 g magnesium nitrate hexahydrate in 50 ml nano-pure water were used. After subsequent drying, samples were calcined at 300 °C for 2 h, followed by cleaning with nano-pure water and then dried at ambient temperature. Calcination at 300 °C was performed to allow the crystallization of the surface [36].

Another immersion process was carried out where magnesium nitrate hexahydrate solution with a concentration of 0.6g was stirred at 35°C for 2 h following Route 2 for the sequence of calcination and cleaning process.

Single-Step Anodization (SSA) Method:

Single-step anodization was performed at voltage of 20 V and two different time periods of 45 and 70 minutes. Precleaned polished titanium was used as anode and platinum foil was used

as cathode. For 45 minutes time periods, electrolyte was 1 vol% HF with a concentration of 1.0 g ($Mg(NO_3)_2 \cdot 6H_2O$) used, and for 70 minutes time periods, electrolyte was 1 vol% HF with three different concentrations of ($Mg(NO_3)_2 \cdot 6H_2O$): 0.3, 0.8 and 1.0 g. Following the anodization, samples were rinsed with nano-pure water and dried at ambient temperature. Finally, calcination of Mg-deposited Ti samples was carried out at 450°C for 1 h a rate of 5°C/ min [46].

Reverse Polarization Process:

Reverse polarization was performed in 50 ml electrolyte solution containing 0.6 g and 1.0 g of $Mg(NO_3)_2 \cdot 6H_2O$ at voltage of 3V for 45 s. Titanium and platinum (Pt) foil were used as cathode and anode, respectively. Similar to immersion method, two different routes were used to study the effect of furnace drying on surface topography and doping content. In the first route, samples were dried in furnace at 90 °C for 2 h, followed by cleaning with nano-pure water and calcined at 450°C for 1 h a rate of 5°C/ min [46]. In the second route, samples were cleaned with nano-pure water after reverse polarization process and then calcined at 450°C for 1 h a rate of 5°C/ min [46].

In another method, anodic oxidation was carried out after the reverse polarization process to investigate the effect of surface topography and doping content. Upon reverse polarization process, anodic oxidation was carried out in the electrolyte of 1.0 g $Mg(NO_3)_2 \cdot 6H_2O$ at voltage of 3 V and two different time periods of 45 s and 5 mins, whereas titanium was used as anode and platinum (Pt) foil was used as cathode. After anodic oxidation process, sample was cleaned with nano-pure water and calcined at 450°C for 1 h a rate of 5°C/ min [46].

Material Characterization:

Surface morphology was evaluated by using field emission scanning electron microscope (FESEM, Hitachi model S4500) and elemental deposition was performed by using energy dispersive spectroscopy (EDS, Oxford Instruments).

2.3 Results and Discussion

2.3.1 Results

Figure 10 shows the morphology of the samples prepared by immersion method and first route, which includes the cleaning of samples after drying, followed by calcination at 300 °C. SEM analysis showed successful anodization and nanotube formation; however, no particulate-like structure resembling Mg deposition was found on nanotubes, which was in line with our EDS evaluation, where no Mg was present.

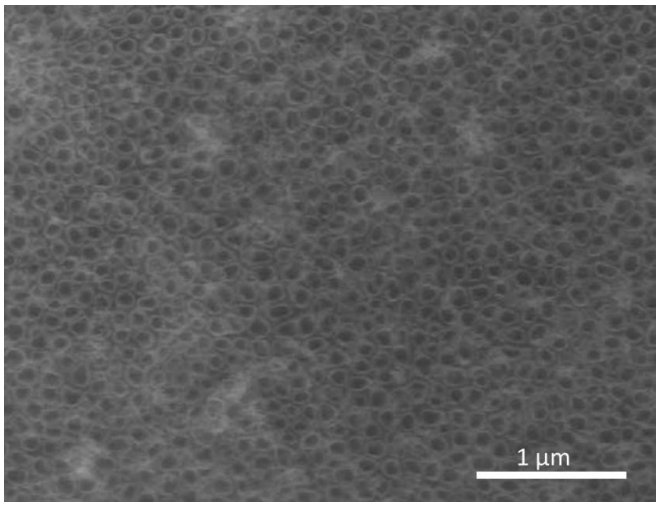

Figure 10: Surface morphology of TiO_2 nanotube without Mg doping.

In samples with immediate calcination after drying, not only nanotubular structure but also Mg particles deposition was confirmed by both SEM and EDS analysis. Mg particles were deposited mainly on and between the walls of the nanotubes and higher deposition rate was found in samples immersed in 1.0 g of Mg $(NO_3)_2 \cdot 6H_2O$ solution, as compared to the 0.6 g. Mg content of 0.81 wt% ± 0.15 wt% and 1.8 wt% ± 0.12 wt% that were measured for 0.6 and 1.0 g of Mg $(NO_3)_2 \cdot 6H_2O$ immersion solution respectively. The highest deposition rate of 10.96 wt% ± 1.48 wt% was found on samples with immersion concentration of 2.0 g, which shows significant increase in deposition with slight increase in precursor concentration, is in line with SEM data where the majority of surface is covered by particles.

Samples prepared by immersion method, where magnesium nitrate hexahydrate solution with a concentration of 0.6g was stirred at 35°C for 2 h instead of 0.5 h, followed Route 2 for the sequence of calcination and cleaning process. SEM analysis showed that nanotubes formed successfully throughout the surface and Mg particles also deposited on and between the wall of the nanotubes, and no significant difference of Mg content was observed compared to the short time duration (0.5h) of stirring period of immersion solution. The Mg content of 0.6 wt% ± 0.1 wt% was found with immersion solution stirring period of 2 h.

Figure 11 shows the morphology of the samples prepared by immersion methods and Route 2 that includes calcination of samples at 300°C after drying followed by cleaning of the samples (a-c); figure 11 also shows samples when immersion solution was prepared by stirring at 35°C for 2 h (d).

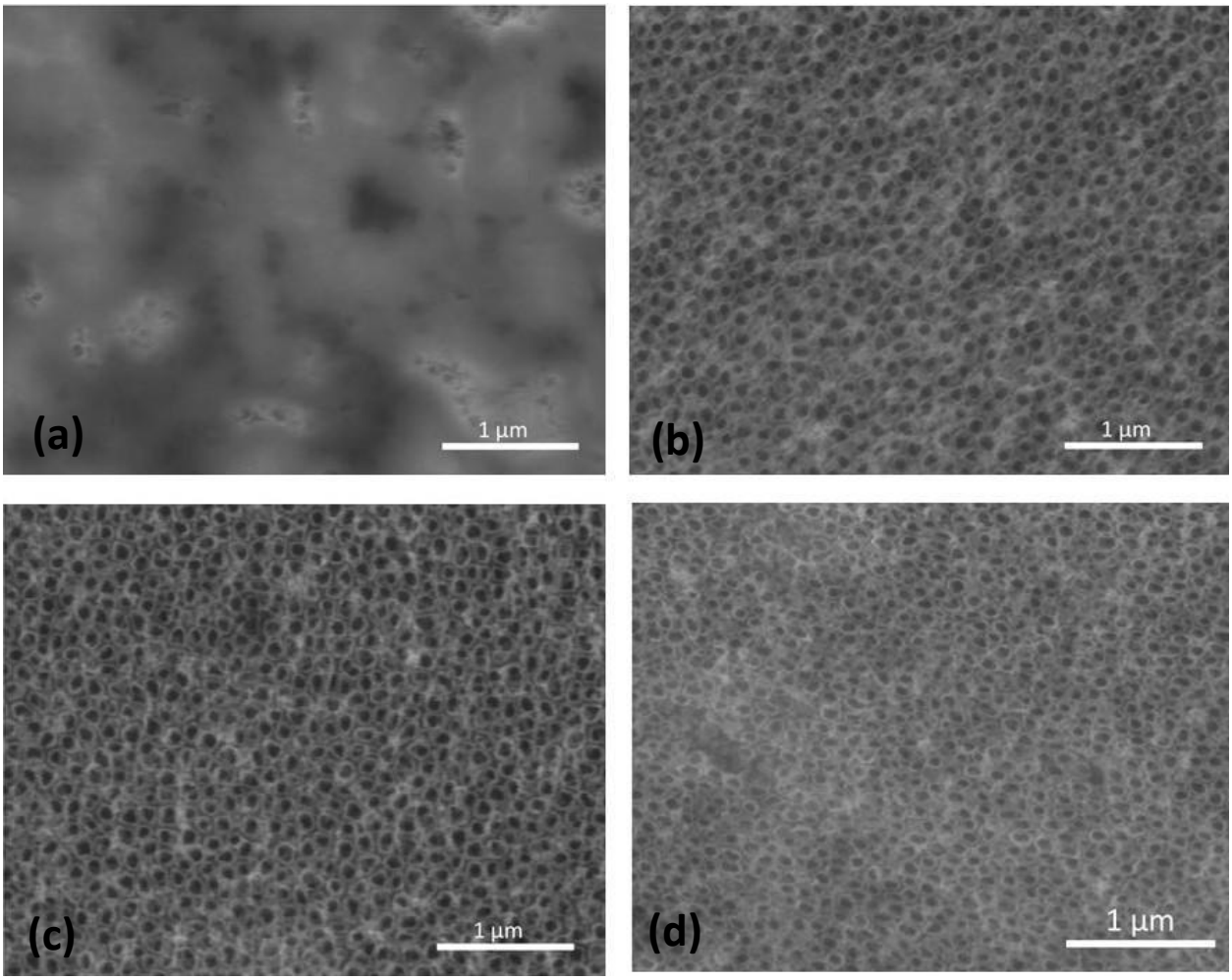

Figure 11: Surface morphology of Mg-doped TiO_2 nanotube obtained under different Mg $(NO_3)_2 \cdot 6H_2O$ concentrations. (a) 2.0 g (b) 1.0 g (c) 0.6 g, and (d) 0.6 g Mg $(NO_3)_2 \cdot 6H_2O$ solution was stirred at 35 °C for 2 h.

Figure 12 shows the morphology of the samples prepared by single-step anodization method at voltage of 20 V and two different time periods of 45 and 70 minutes. For both time periods of single-step anodization, SEM analysis showed successful anodization and nanotube formation, but Mg particles as well as residue formed due to incomplete chemical reaction which covered the surface of the nanotubes. According to EDS analysis, Mg content of 0.4 wt% ± 0.1 wt% was measured on samples with a concentration of 1.0 g Mg $(NO_3)_2 \cdot 6H_2O$ when single-step anodization was carried out for 45 minutes, whereas Mg content of 0.59 wt% ± 0.10 wt%, 0.76

wt% ± 0.11 wt% and 0.9 wt% ± 0.15 wt% were measured for 0.3 g, 0.8 g and 1.0 g respectively, when single-step anodization was performed for 70 minutes.

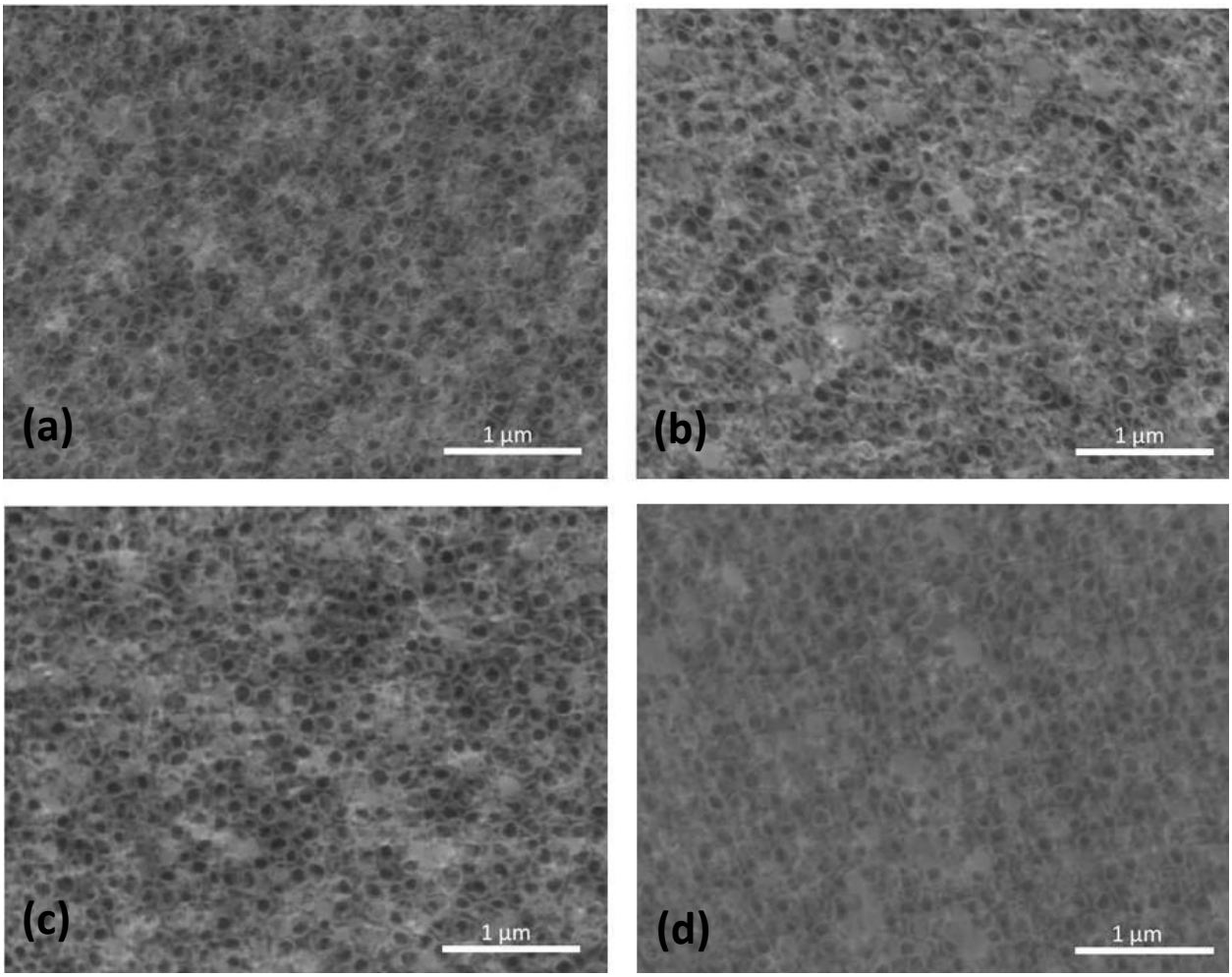

Figure 12: Surface morphology of Mg-doped TiO_2 nanotube obtained when anodization was performed for 70 minutes in three different Mg $(NO_3)_2 \cdot 6H_2O$ concentrations. (a) 1.0 g (b) 0.8 g (c) 0.3 g, (d) Surface morphology of Mg-doped TiO_2 nanotube obtained when anodization was performed for 45 minutes in 1.0 g Mg $(NO_3)_2 \cdot 6H_2O$ concentration electrolyte solution.

Figure 13 (a-b) shows the morphology of the samples prepared by reverse polarization method and Route 1, which includes furnace drying after the reverse polarization process, followed by cleaning and finally calcined at 450 ℃. SEM analysis showed precipitation on the nanotube surface and magnesium doping was confirmed by EDS analysis. Mg content of 3.42 wt % ± 1.01 wt% and 1.97 wt% ± 0.44 wt% was measured for 1.0 g and 0.6 g Mg $(NO_3)_2 \cdot 6H_2O$ concentrations, respectively.

In samples with immediate cleaning after reverse polarization followed by calcination at 450 ℃, surface morphology was found similar to Route 1 as shown in Figure 13 (c-d). The total magnesium content of 2.59 wt% ± 0.40 wt% and 1.47 wt% ± 0.48 wt% was found on samples with concentrations of 1.0 g and 0.6 g.

Figure 13 (e-f) shows surface morphology of the samples prepared by reverse polarization followed by anodic oxidation at two different time periods of 45 s and 5 minutes, respectively. The nanotubes surface with precipitate as well as Mg deposition were confirmed by SEM and EDS analysis. Mg content of 3.13 wt% ± 1.04 wt% and 1.40 wt% ± 0.43 wt% were measured for 45 s and 5 minutes periods of anodic oxidation, respectively.

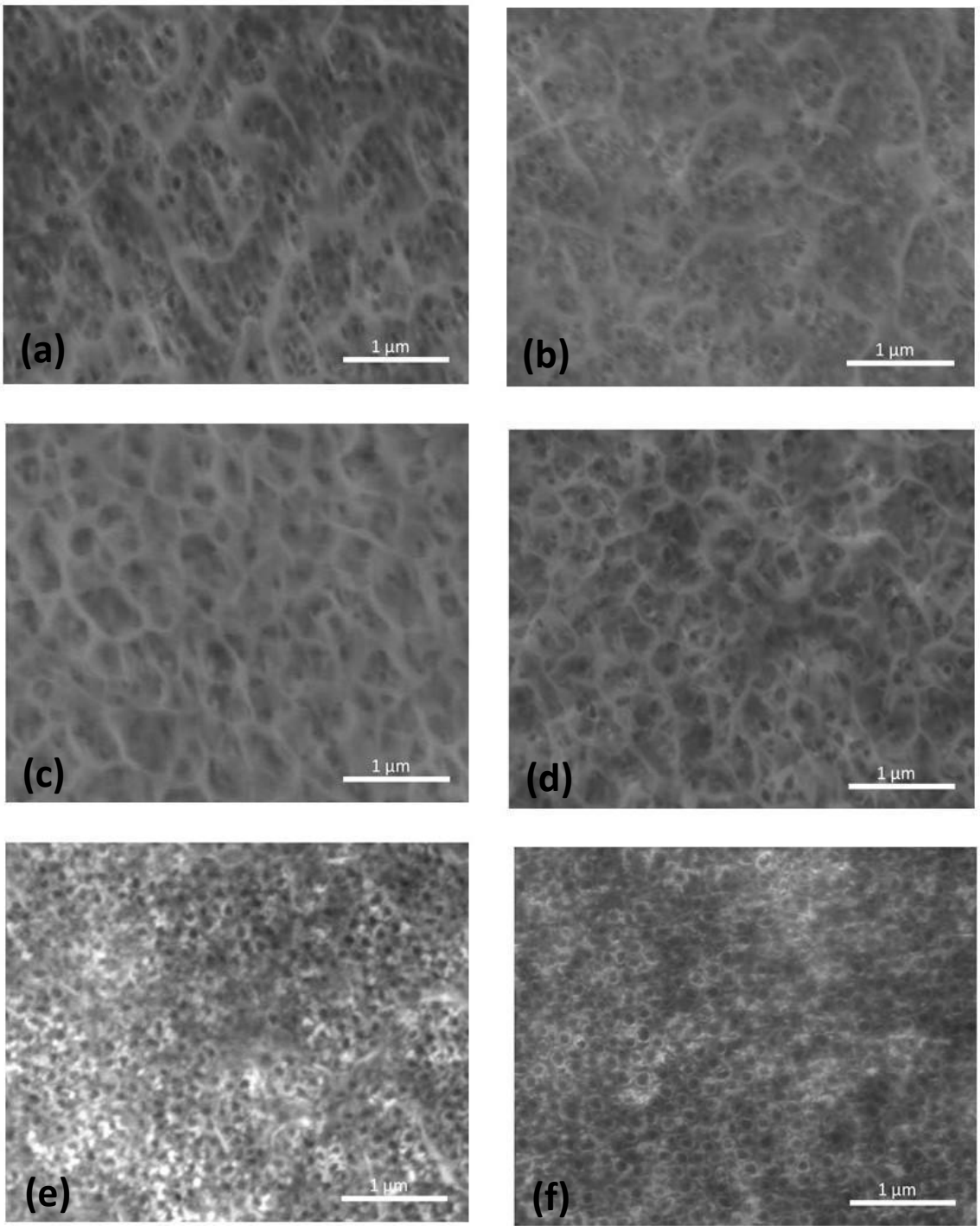

Figure 13: (a-b) Surface morphology of samples that include the furnace drying after the reverse polarization process, followed by cleaning for 1.0 g and 0.6 g of Mg $(NO_3)_2 \cdot 6H_2O$ respectively, (c-d) Surface morphology with immediate cleaning followed by calcination for 1.0 g and 0.6 g of Mg $(NO_3)_2 \cdot 6H_2O$ respectively, (e-f) Surface morphology when anodic oxidation was carried out after reverse polarization at 45s and 5 minutes, respectively at 1.0 g of Mg $(NO_3)_2 \cdot 6H_2O$.

2.3.2 Discussion

TiO_2 nanotubes are of great interest in orthopedic and dental applications because of high surface compared to flat titanium, which increases additional space for cellular interaction [92]. In this study, magnesium was incorporated into nanotubes and nanostructures using different experimental techniques. Anodization was carried out to get bone-inspired surface morphology. Research found that the formation of TiO_2 nanotubes enhances bone mineralization's compared to non-nanotexturised titanium surfaces [93]. The nanotube was formed by anodization of a Ti smooth surface following two steps: 1) field-assisted oxidation to form TiO_2 passive layer on Titanium smooth surface by the recombination of Ti^{4+}, $O^{2-}$and OH^- ions due to the action of electric potential and 2) chemical dissolution of passive oxide layer by F^- ion and finally forming pits. The consequence of oxidation and dissolution process results is the formation of nanotubes from nanopores [21, 94-96]. The reactions of forming nanotubes by anodization are given below [97]:

$$Ti + 2H_2O \rightarrow TiO_2 + 4H^+ + 4e^-$$

$$TiO_2 + 4H^+ + 6F^- \rightarrow TiF_6^{2-} + 2H_2O$$

In response to immersion method for incorporating magnesium into the TiO_2 nanotubes, various routes were performed for post-processing of samples after furnace drying, as explained in the experimental procedure section. The samples with immediate calcination after furnace drying followed by cleaning showed satisfactory surface morphology with Mg doping on and between the wall. A study was performed on silver deposition into titanium nanotubes by pulse current deposition (PCD) methods where silver was deposited on and between nanotubes as well as at the bottom of the nanotubes [78]. The trapped air in the TiO_2 nanotube was removed due to

the immersion of the nanotube samples into the solution, which facilitates direct contact of magnesium nitrate solution with the nanotube network, and Mg^{2+} was adsorbed by the TiO_2 nanotube surface. In addition, increasing the time deposition of titanium substrate into the solution leads to the deposition reaction of forming $Mg(OH)_2$ colloid from Mg^{2+} ion and adhering to the nanotube surface. This $Mg(OH)_2$ colloid transformed into MgO when the titanium substrate was heated at 300 ºC for 2 h to dehydrate the substrate. Thus, the excess Mg^{2+} was doped into the TiO_2 nanotube lattice structure [87]. If concentration of $Mg(NO_3)_2 \cdot 6H_2O$ is reduced in immersion solution, then colloidal form of $Mg(OH)_2$ will decrease, resulting in less doping of Mg^{2+} ion into the lattice structure. From EDS results, it was also found that when there was a decrease in concentration of $Mg(NO_3)_2 \cdot 6H_2O$ into the immersion solution, Mg^{2+} deposition rate also decreased.

The single-step anodization technique was another method used to incorporate magnesium in the modified surface. The anodization was carried out at a voltage of 20 V and two different time periods of 45 minutes and 70 minutes. Research showed that the deposition of ions can be controlled by the concentration of initial ion solution and pore size [72]. Loading capacity of the nanotubes increased with the increase of Mg^{2+} ion content in the solution [72]. Figure 12 (a-d) above shows the surface morphologies of magnesium-doped titanium modified surface at different conditions. At all concentrations and conditions, Mg was doped into the nanotubes, but large amounts of precipitates formed on and between the nanotubes. Nanotubes formation was carried out in two steps: 1) formation of oxide layer and 2) chemical dissolution of oxide layer by F^- and forming pits. Due to the addition of magnesium nitrate hexahydrate ($Mg(NO_3)_2 \cdot 6H_2O$), Mg^{2+} ion was present in the electrolyte solution at higher concentration compared to F^- ion, resulting in the

lack of free F^- as a consequence of the reduction of dissolution reaction, which formed stain-like structures on the surface [98].

Mg deposition depends on anodization period. Mg incorporation was increased due to the enhancement of anodization period, which was confirmed by EDS result. In samples with a concentration of 1.0 g Mg $(NO_3)_2 \cdot 6H_2O$, Mg deposition rate was higher for 70 mins anodization period compared to 45 mins.

Reverse polarization was another method of magnesium deposition into the titanium-modified surface. TiO_2 film undergoes various stages from oxide reduction reaction to dissolution and the processes are adsorption and absorption of hydrogen, hydrogen evolution and oxygen reduction reaction [94]. When TiO_2 nanotubes were introduced to reverse polarization, TiO_2 nanotube film's thickness was reduced due to the influence of hydrogen evolution reaction [94, 99]. This hydrogen evolution reaction caused the reduction of Ti^{4+} ion in TiO_2 film to Ti^{3+}, resulting in the reduction of TiO_2 to TiOOH [39,40]. Due to the dissolution of TiO_2 film in electrolyte, precipitates formed on the nanotube surface [94].

2.4 Conclusion

In this study, various deposition methods were used to incorporate magnesium into titanium-modified surface. The results found that nanotubular structure with successful deposition of magnesium occurred by immersion methods followed by subsequent drying and calcination. The magnesium content increased with the increase of magnesium nitrate hexahydrate concentration in the immersion solution. The magnesium deposition also performed by single-step anodization technique where less amount of magnesium also deposited as well as residual formed on the titanium-modified surface. In response to the reverse polarization technique, magnesium

was deposited on the surface as well as precipitate formed on the surface which covered the nanotubes. The magnesium content by reverse polarization was higher compared to other methods. Thus, magnesium deposition with well-developed nanotube structures was formed by immersion method followed by subsequent drying and calcination process.

CHAPTER 3 CONTROLLED RELEASE OF ALOE-EMODIN FROM SURFACE-MODIFIED TITANIUM AND ITS *IN VITRO* INTERACTION WITH HUMAN OSTEOBLAST CELLS

3.1 Introduction

Titanium is one of the most promising metals used in bone metabolic disease treatment due its biocompatibility, high mechanical strength and high corrosion resistance behavior [100, 101]. Chronic bone metabolic diseases like osteopenia and osteoporosis are usually common among older people [101]. The term “osteopenia” means low bone mass due to lower bone density; osteoporosis alters trabecular bone strength resulting in the reduction of bone regeneration [101]. Both diseases cause the failure of implants which can be reduced by enhancing osteointegration between bone and implant [100, 101]. The strong oxide layer on the titanium surface makes the surface bio-inert, which inhibits the bone and implant interaction [100]. The lack of osteointegration is more complex for patients who are suffering osteosarcoma [101]. Osteosarcoma is the bone tumor most likely derived from mesenchymal stem cells [102]. In 80% of the cases, osteosarcoma occurs in metaphysis of the long bone, although it may also occur in diaphysis of long bone and axial skeleton [103]. To increase the osteointegration, surface modification techniques are necessary to alter surface topography and increase surface roughness, physically mimicking host bone structure and improving biocompatibility of the implant [104,105]. Surface roughness enhances contact area of the implant and has direct effect of osteoblast cell proliferation and differentiation [104]. The osteoblastic adhesion is essential for

maintenance of tissue integration, wound healing and biomaterial tissue integration [106]. Research shows that higher surface roughness promotes higher osteoblast cell proliferation and attachment [106]. In addition, several studies showed that osteosarcoma cell (MG-63) adhesion, proliferation rate, differentiation and growth factor production are influenced by rough surface of the titanium [107, 108].

An implant is a bio-inert device that is used for bone repair, support or therapy, but the purpose of the implant may be extended because of technical and therapeutic reasons [109]. Implantable drug delivery devices have been classified into two categories: active and passive [109, 110]. The former category can be controlled by external drives or stimuli, while in the second category, the drug release cannot be controlled after implantation [109, 110]. Passive implants can be biodegradable or non-biodegradable [109, 110]. Oral drug delivery system is one of the most widely used drug delivery systems because of dose accuracy, simplicity of use and ease of treatment termination [110, 111]. However, it has many disadvantages: degradation in acidic condition of stomach or alkaline condition of intestine, poor intrinsic permeability, possibility of enzymatic attack, and damage of non-targeted cells [61, 110, 112]. Localized drug delivery system is the alternative way to reduce infection of the surgical area, reduce toxicity in non-targeted cells and enhance deposition in tumor [61, 113, 114]. However, drug release from the implant must be in an optimal manner in the implant area [115]. The drug molecules can be released from the implant by different mechanisms for a certain period and facilitate the technical features of the implant [116].

Sustained drug release from the implant prevents adverse effects in the implant area [115], keeps the drug concentration at constant rate in the target tissue [116], ensures the drug delivery

for long periods of time [116] and improves efficacy of the treatment [117]. Sustained drug release is beneficial especially for cancer treatment [116]. Sustained drug release can be achieved by prohibiting the drug molecule into the aqueous environment by controlling the diffusion rate of the drug molecules or by adjusting the degradation speed of the carrier [116]. Different methods are used for sustaining drug release: polymer-based drug delivery system [109], dynamic implant system like osmotic pump system, implantable pump system [115], electromechanical system [115], and ion exchange resin drug delivery system [118].

Biodegradable polymers like gelatin, chitosan, polycaprolactone, poly(lactic acid) and poly(lactic-co-glycolic acid) (PLGA) are widely used to apply coating on drug-loaded metallic implants, where drug molecules are released from polymer matrix by diffusion [119]. Polymer is coated into the drug-loaded implant by different methods: dip-coating technique [120], drop-wise method [61], and solvent-casting methodology [121]. PLGA is one of the most commonly used polymers because of its desired degradation properties, biocompatibility, good mechanical strength, hydrophobic/hydrophilic balance and crystallinity [113, 122, 123]. PLGA is a liner co-polymer composed of its monomers, lactic acid (LA) and glycolic acid (GA). PLGA is obtained through a polymer synthesis process with different lactic acid and glycolic acid ratios [123]. Depending on the ratio, the degradation properties of the PLGA varies. PLGA with higher lactic acid (LA) concentration has lower degradation rate [123]. Thus, higher LA concentration means lower dissolution rate as well as degradation rate.

Aloe-emodin, a hydroxyanthraquinone [124], is a natural compound extracted from leaves of aloe vera [125] and from the roots and rhizomes of *Rheum palmatum L* [126] that is used for multiple applications such as antifungal activity [127], antitumor or anticancer [124], and anti-

inflammatory response [128]. In addition, emodin increases osteoblast differentiation at low concentration by inducing BMP-2 gene expression via activating the PI3K-Akt and/or MAP kinase–NF-κB signaling pathways [129]. A study showed that aloin, another anthraquinone extracted from aloe vera, accelerated osteogenic induction of MC3T3-E1 cells [130]. Another study indicated that acemannan was used to investigate its effect on load-bearing applications where acemannan was extracted from aloe vera gel by ethanolic Soxhlet extraction procedure [131]. However, the effects of aloe-emodin (AE) on drug release kinetics, *in vitro* cell proliferation, and attachment have not been examined.

The aim of this study is to examine the effect of aloe-emodin (AE) in PLGA-coated titanium nanotubes on release kinetics and *in vitro* osteoblast cell viability. Titanium nanotube samples were prepared by anodization process. AE was loaded on samples followed by PLGA coating at different concentrations of lactic acid and glycolic acid. To validate the hypothesis, *in vitro* release of AE was investigated in phosphate buffer solution (pH 7.4) and acetate buffer solution (pH 5.0) from both PLGA-coated and non-coated samples. Cell attachment and proliferation were studied based on the effect of AE, presence of PLGA coating and cell culture period. Based on drug-polymer interaction, surface chemistry of metal and environment, it is believed that AE could lead to a beneficial effect on *in vitro* cell viability that will accelerate bone formation.

3.2 Materials and Methods

3.2.1 Materials

Commercially pure titanium (cp-Ti grade #2, President Titanium, MA, USA), ethanol (200 proof anhydrous), acetone (certified ACS), hydrofluoric acid (48-51% solution in water), aloe-

emodin (≥95% HPLC, MW:270.24 g/mol, purchased from Sigma Aldrich, St. Louis, MO, USA), PLGA (LA:GA- 50:50, 65:35, 75:25, purchased from Sigma Aldrich, St. Louis, MO, USA) and dimethyl sulfoxide (DMSO).

3.2.2 Methods

Preparation of TiO_2 Nanotubes:

Commercially pure titanium disks with a diameter of 11 mm and a thickness of 2 mm were ground by silicon abrasive paper (grits 320, 400, 600 and 800), followed by polishing (using MasterTex polishing cloth). Samples were then washed and cleaned by DI water, ethanol, acetone and finally dried at ambient temperature.

TiO2 nanotubes were formed by anodization process as explained in detail in our previously published work [91]. Briefly, anodization was carried out in 1 vol. % HF electrolyte solution at 20 V for 45 minutes; titanium disk and platinum foil were used as anode and cathode, respectively. After anodization, titanium substrate was rinsed with DI water and dried at atmosphere.

Incorporation of Aloe-Emodin:

Aloe-emodin (AE) drug was dissolved in dimethyl sulfoxide (DMSO) with a ratio of 50 mg/ 1ml DMSO. After dissolution in DMSO, the liquid drug solution was diluted into DI water based on loading concentrations. In this experiment, 60 µL liquid drug-DMSO-DI water solutions were loaded in each titanium substrate to get 100 µg AE in each substrate. Liquid drug solution was loaded in two different types of titanium substrates: polished titanium and titanium nanotubes. The drug-loaded substrates were then dried completely at room temperature.

Polymer Coating on Aloe-Emodin-Loaded Titanium Substrates:

Three different types of PLGA with ratios of 50:50, 65:35 and 75:25 lactic acid (LA) and glycolic acid (GA) were used to coat the aloe-emodin-loaded titanium substrates; 5wt% of three different PLGA solutions were prepared by dissolving each composition in acetone and loaded on titanium substrate, followed by drying at room temperature.

Drug Release Experiment:

Two different types of buffer solutions were used to measure the release of aloe-emodin (AE). A phosphate buffer pH-7.4 was used to mimic physiological pH and acetate buffer was used to mimic the condition just after surgery [132]. Two samples of each type of substrate (polished titanium [cp-Ti] and titanium nanotubes [Ti-NT]) with or without PLGA of different lactic acid and glycolic acid were placed in 4 ml of phosphate buffer and acetate buffer separately. Vials were labelled based on sample types and number, pH; PLGA ratio depends on LA and GA concentrations. Vials were kept in a shaking incubator at 37°C under the speed of 70 rpm. Buffers were collected after 3h, 6h, 12h, 1 day, 2 days, 4 days, 6 days, 8 days, 12 days and 16 days and refilled with fresh buffer solution. Three hundred microliters from each sample in triplicate was pipetted to a 96-well plate and release rate was measured by UV visible spectrometer at a wavelength of 410 nm.

***In Vitro* Cell Material Interaction:**

To understand the effects of aloe-emodin release from titanium on proliferation of bone forming, human fetal osteoblast cells (hFOB 1.19, ATCC CRL-11372TM) were used. The culture medium used for osteoblast cells was a mixture of 1:1 Ham's F12 medium and Dulbecco's modified eagle's medium (DMEM) with 2.5 mM-glutamine (without phenol red; Sigma)

supplemented by 10 % fetal bovine serum (FBS, ATCC), 1.2 g/L of NaHCO3 (Sigma), 0.3 mg/ml G 418 (Sigma) and penicillin/ streptomycin (Invitrogen, Germany) (10 mg/ml). Cells were cultured in 75 cm^3 vented cell culture flasks and maintained at 34 °C under an atmosphere of 5% CO2/ 95% air. Prior to cell culture, titanium nanotube (Ti-NT) substrates were autoclaved to sterilize. Upon sterilization of Ti-NT substrates, 2 µg aloe-emodin (AE) drug was loaded in Ti-NT substrates. After drying, 60 µl of 5% (wt/v) PLGA (LA:GA-65:35) were added onto each of the AE-loaded substrates and dried completely before cell seeding. A total four different types of samples were used: No AE + No PLGA, No AE+ PLGA, AE+ No PLGA and AE+ PLGA. Cells were seeded with a density of $5x10^4$ cells/substrate.

Cell Viability Assessment Using MTT Assay:

The MTT assay was performed after 2, 5 and 7 days of incubation to analyze the efficacy of AE on osteoblast cells. The MTT (Life Technologies, Eugene, OR) solution of 0.5 mg/mL was prepared by dissolving MTT in sterile filtered PBS; 100 µL of MTT solution were added to each substrate in the well plate, followed by 900 µL cell media addition and incubated at 34°C for osteoblast cells. After 2 h of incubation, the media was removed and 600 µL of solubilizer solution (composed of 10 % Triton X, 0.04 M HCl and isopropanol) were added to each substrate to dissolve formazan crystals. One hundred microliters solution were transferred to 96-well plate and read by UV visible spectrometer at a wavelength of 570 nm. Triplicate samples according to composition were evaluated and three measurements were performed from each substrate.

Cell Morphology Imaging:

The cellular morphology was evaluated by field emission scanning electron microscope (FESEM). The substrates were removed from culture at 2, 5, and 7 days. Substrates were fixed in

2% paraformaldehyde/2% glutaraldehyde in 0.1 M phosphate buffer solution and kept overnight at 4 °C. Samples were rinsed with 0.1 M phosphate buffer three times, followed by post fixation with 2 % osmium tetroxide (OsO_4) for 2 h at room temperature. Samples were then rinsed again with 0.1 M phosphate buffer and dehydrated in ethanol series (30, 50, 75, and 100 % three times). Samples were dried overnight and the palladium coating was then used to apply a layer of coating with thickness of 4-5 nm.

3.3 Results and Discussion

3.3.1 Results

Figure 14 shows the cumulative release of AE from polished and anodized (or NT) titanium samples with or without PLGA coating at pH- 7.4. The drug release rate from both types of samples without PLGA coating was higher than the PLGA-coated samples. At initial stage, burst release of AE occurred within the first 2 days, and almost 70% and 60 % of the drug was released from polished and anodized samples with no polymer coating, respectively, and plateaued after that. The presence of PLGA coating decreased the AE release. For polished samples with PLGA coating, AE release decreased with the increase of lactic acid concentration in PLGA as shown in Figure 14 (a). However, the release of AE increased from PLGA-coated (75:25) polished samples compared to PLGA-(65:35) and PLGA-coated (50:50) polished samples after 50 and 148h, respectively. Almost 77%, 70% and 83% of AE was released from polished samples coated with PLGA (50:50), PLGA (65:35) and PLGA (75:25), respectively, after 16 days. On the other hand, the AE release from anodized samples with PLGA coating decreased with the increase of lactic acid concentration in the PLGA, as shown in Figure 14 (b). There was almost 73%, 53% and 48% of AE release from the anodized samples coated with PLGA (50:50), PLGA (65:35) and PLGA

(75:25), respectively, after 16 days. Figure 14 (a) and Figure 14 (b) show that release of AE from the polished samples coated with PLGA was higher than release from the anodized (or NT) samples coated with PLGA.

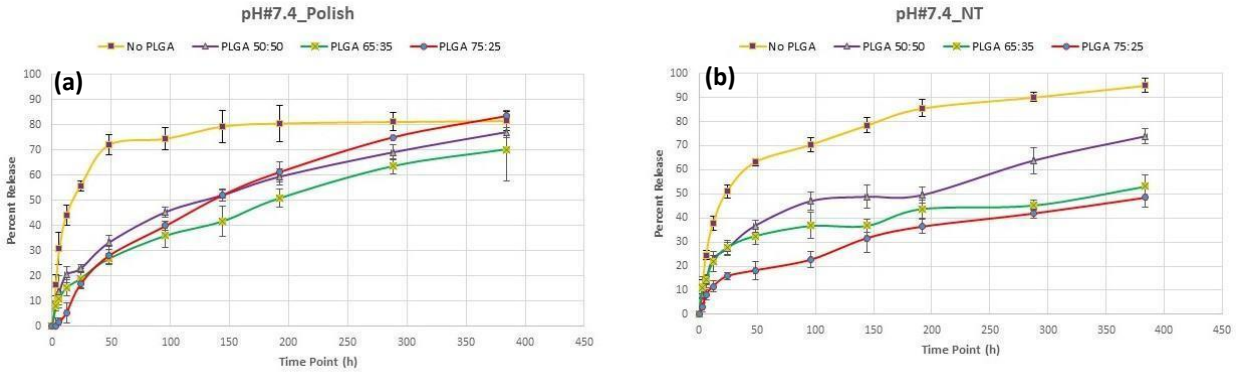

Figure 14: Percentage release of AE from samples with and without PLGA coating at pH-7.4. (a) Polished samples, (b) Anodized (or NT) samples.

Figure 15 shows the cumulative release of AE from polished and anodized samples with or without PLGA coating at pH-5.0. In both types of samples without PLGA coating, the AE release was higher compared to the samples with PLGA coating. An initial burst release of AE occurred within the first 2 days, and nearly 64% and 63% of AE was released from polished and anodized samples, respectively. The presence of PLGA coating decreased AE release significantly. The AE release decreased with the increase of lactic acid concentration in PLGA from both types of samples, but cumulative release of AE was lower in anodized samples compared to polished samples. AE release from anodized samples with PLGA (75:25) coating was almost the same as PLGA-coated (65:35) anodized samples. After 16 days, there were almost 54%, 51% and 28% of AE released from PLGA-(50:50), PLGA-(65:35) and PLGA-coated (75:25) polished samples, respectively, while around 47%, 33% and 33% of AE was released from PLGA-(50:50), PLGA-(65:35) and PLGA-coated (75:25) anodized samples, respectively.

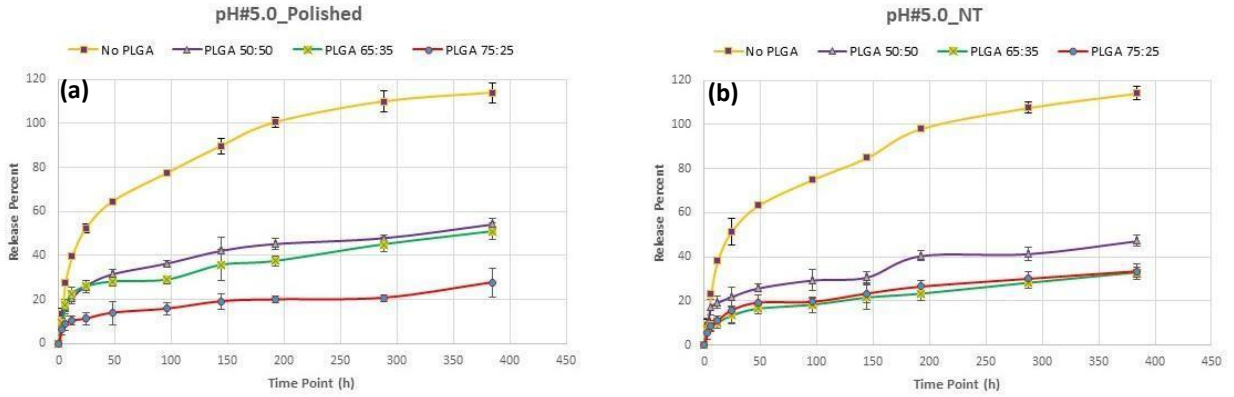

Figure 15: Percentage release of AE from samples with and without PLGA coating at pH-5.0. (a) Polished samples, (b) Anodized (or NT) samples.

Figure 16 shows the osteoblast cell viability by MTT assay and cell morphology by SEM after 2, 5, and 7 days of culture. Flattened adhere cells with filopodia were observed on the No AE+ No PLGA, No AE+ PLGA, AE+ NO PLGA and AE+ PLGA samples after 2 days of culture. Figure 16a shows that there was no significant cell proliferation in AE-loaded nanotube samples compared to non-AE-loaded nanotube samples after 2 days. However, cell viability was found almost similar for AE loaded with polymer-coated nanotube samples and non-AE-loaded polymer-coated nanotube samples. After 5 days of culture, cell viability was reduced on AE loaded with and without PLGA-coated nanotube samples compared to non-AE-loaded nanotube samples. The cell viability of AE-loaded nanotube samples was higher than the non-AE-loaded nanotube samples after 7 days of culture. A coating of PLGA controlled the release kinetics of AE and reduced the cell viability. Excellent cell attachment was noticed on No AE+ No PLGA, No AE+ PLGA, AE+ No PLGA and AE+ PLGA titanium nanotube samples after 5 and 7 days of culture, as shown in Figure 16b.

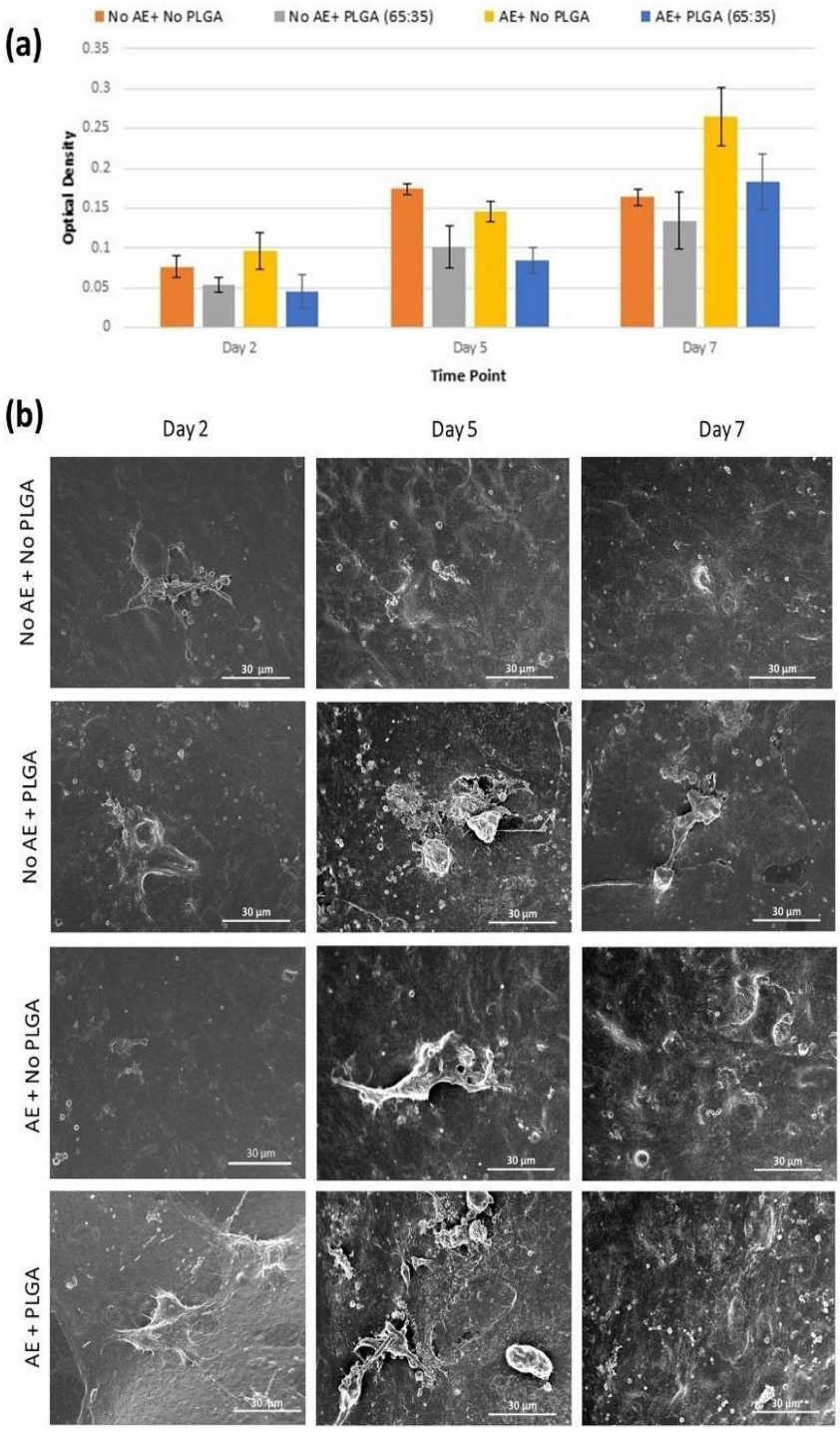

Figure 16: a) *In vitro* osteoblast cell viability of AE and No AE loaded with and without PLGA-coated titanium nanotube samples after 2, 5, and 7 days of culture, b) SEM micrograph of osteoblast cell attachment of AE and No AE loaded with and without PLGA-coated titanium nanotube samples.

3.3.2 Discussion

Many plant-derived natural medicinal compounds are used in orthopedic applications to stimulate bone formation [129- 131]. AE is a natural hydroxyanthraquinone, especially used in anticancer or antitumor therapy [124, 133]. Previous research showed that AE was also used to inhibit diseases to vascular calcification *in vitro* and *in vivo* [134]. The aim of this research study was to investigate the effect of control release of AE from surface-modified titanium on osteoblast cell viability and proliferation.

Titanium has been used as a metallic implant in hard-tissue applications because of its biocompatibility [135]. However, due to its bio-inertness behavior, surface modification is necessary [18]. The surface modification by anodization increases surface roughness and produces a thicker oxide layer that enhances bone response to titanium [136]. The drug molecules are attached to the surface of biomaterials due to strong electrostatic interaction between a porous surface and drug molecules [132, 137, 138]. This electrostatic interaction can be suspended due to the stronger interaction between released media and drug particles, resulting in the uncontrolled release of drug molecules from the samples [132]. Initial burst release or uncontrolled release is the common phenomena that could damage target tissues [132, 137]. Therefore, sustained drug release is necessary to get the efficacy of treatment for a period of time [61, 138]. Previous research showed that drug delivery from biodegradable polymer coating controlled the release rate, resulting in the beneficial effect of treatment [132, 138]. In this study, PLGA was used as coating on the drug-loaded polished titanium and titanium nanotube samples due to its nontoxic effect while degrading it into the body [120]. Our results showed that release of AE from both polished and anodized (or NT) samples were different based on the constituent monomeric ratios (lactic

acid and glycolic acid) of the PLGA. Results showed that the cumulative AE release decreased with the increase of lactic acid concentration in PLGA. The reason behind this scenario was that higher concentration of lactic acid (LA) in PLGA causes lower degradation rate, i.e., higher dissolution rate into the release media [123]. Glycolic acid (GA) is more hydrophilic; thus, lower concentration of GA means lower dissolution rate of PLGA [123]. PLGA starts degradation by hydration process, which involves water penetration in the amorphous region, resulting in the weakening of van der Waals forces and hydrogen bond, followed by the initial degradation by fission of covalent bond and continuous degradation by mass fission of the backbone of covalent bond [123]. As a result, the fragments are further split into molecules that are soluble in aqueous environment [123]. The diffusion kinetics also depend on diffusion, matrix degradation and external or electronic processes [61, 138].

The AE forms hydrophobic interaction with the PLGA, which controls release rate in pH 7.4 and pH 5.0 [61]. Figure 14 and Figure 15 show a high amount of drug release from the beginning to end of the AE release study at higher pH (pH 7.4) compared to lower pH (pH 5.0). The reason behind the phenomena was the higher interaction between AE and released media compared to the AE and PLGA interaction [132]. Figure 17 below shows favorable and unfavorable interactions between AE and PLGA. At higher pH, AE releases protons and this deprotonated form of AE is more hydrophilic than a protonated form, which caused unfavorable interaction between PLGA and AE, resulting in the release of a high amount of AE at a higher pH (pH 7.4) value [132].

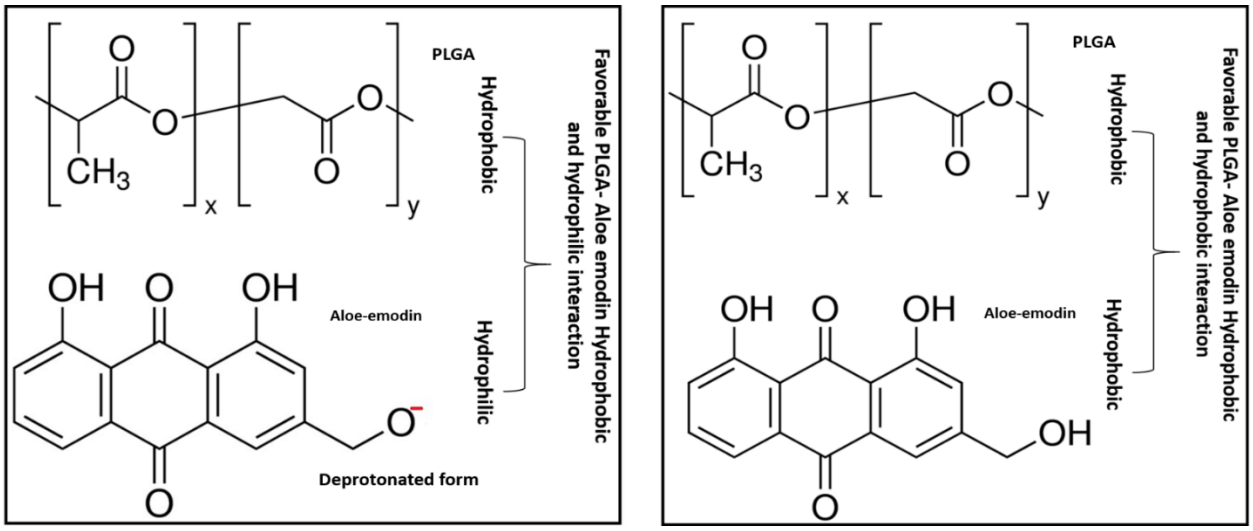

Figure 17: Chemical structural interpretation of hydrophobic-hydrophobic and hydrophobic-hydrophilic interaction between PLGA and AE.

The hydrophobic interaction of PLGA and AE and solubility of PLGA into the release media also influenced the release rate of the AE molecules [132]. As LA is more hydrophobic, therefore, with the increase of LA concentration, AE released from the samples was also reduced, as shown in Figures 14 and 15 for both release media at pH 7.4 and pH 5.0. In addition, surface roughness also had an important role in electrostatic interaction between AE and titanium samples. The sample surface of polished titanium is often smoother, whereas anodized (or NT) sample surface is rougher due to the formation of NT on the surface [136]. Thus, the interaction between polished titanium sample surface and AE was lower, resulting in a higher release of AE from polished samples compared to NT samples. In Figure 14, an opposite behavior was observed on PLGA-coated (75:25) and AE-loaded polished titanium samples. After 2 days, AE release rates from PLGA-coated (75:25) AE-loaded polished samples were higher than the PLGA-coated (65:35) and AE-loaded polished samples, and the release rate increased with the increase of time. Finally, the cumulative AE release from PLGA-coated (75:25) AE-loaded polished titanium

samples was higher than the PLGA-(65:35), and PLGA-coated (50:50) coated AE-loaded polished titanium samples. This happened due to the higher interaction between PLGA and AE compared to the polished surface of titanium and AE that caused the detaching of AE-PLGA (75:25) layer from the polished titanium surface.

The effect of AE on *in vitro* osteoblast cell material interaction has been demonstrated in Figure 16 for a span of 7 days. In Figure 16a, after 5 days of culture, the presence of AE inhibited the cell growth. The inducing of PLGA coating decreased cell inhibition rate of AE-loaded samples by controlling the release rate. After 7 days of culture, cell viability increased due to the presence of AE in both PLGA- and non-PLGA-coated samples. The control release of AE due to PLGA coating decreased cell growth, which revealed the influence of AE release rate on osteoblast cells proliferation. The SEM images also showed flattened adhered cells with filopodia on all types of sample surface. The high OB cell density observed on the AE-loaded samples was compared to non-AE-loaded samples after 7 days of culture, which also correlated with the quantitative analysis of cell viability by MTT assay. Previous research investigated the effect of aloe vera or aloe vera extracted natural compounds on bone healing or bone repairs [131, 139]. A study showed that aloe vera stimulates bone formation, accelerates the repairing process and reduces inflammatory effects. Another study investigated the effects of acemannan, an extracted compound from aloe vera gel, on *in vitro* and *in vivo* biological properties. Results indicated that aloe vera enhances bone formation and accelerates bone healing [131]. In our study, AE is also an aloe vera extracted natural compound and has an anti-inflammatory response. This anti-inflammatory factor facilitates bone formation [139]. Emodin, another anthraquinone natural compound, has also been used for anticancer and anti-inflammatory therapy [18]. Research showed that emodin inhibits osteoclast differentiation and function and stimulates osteoblast formation [18].

The main outcome of this study was the development of a PLGA-coated AE-loaded titanium nanotube implant that can be used as a delivery vehicle for AE release from the implant. The results show that the release of AE from the developed implant stimulates osteoblast cell interaction and proliferation.

3.4 Conclusion

In this research, aloe-emodin (AE), a natural compound extracted from aloe vera, was used to investigate its effect on *in vitro* osteoblast cell growth. Titanium nanotube samples were used to incorporate AE into the nanotube and PLGA coating was applied to control the release rate of drug to get the desired output of the AE. Results shows that the AE-loaded titanium nanotube samples with PLGA coating control the release rate of AE from the samples. The sustained and effective AE release was observed from the titanium nanotube samples coated with PLGA (65:35). An *in vitro* cell culture experiment was performed on human fetal osteoblast cells on AE and No AE-loaded titanium nanotube samples with and without PLGA (65:35) coating. Results shows that the samples with AE load enhance osteoblast cell proliferation and attachment. Thus, the result from this study reveals that effect of AE enhances osteoblast bone formation.

CHAPTER 4 SURFACE MODIFICATION OF TITANIUM BY ALKALI TREATMENT AT DIFFERENT TEMPERATURES AND ROTATIONAL SPEEDS.

4.1 Introduction

Titanium is one of the metals that has been widely used in orthopedic and dental applications because of its biocompatibility and good mechanical properties [5,140]. Biocompatibility is an important characteristic of implants to ensure appropriate host response by emitting toxicity into the surrounding tissues [141]. In addition, mechanical properties like Young's modulus, tensile strength, hardness and elongation have an impact on the implant's lifetime [5]. To enhance implant lifetime, the mechanical properties of the implant and bone are expected to be similar [5]. Osteointegration is another property that increases the interaction between the implant and surrounding tissue, thus enhancing the lifetime of the implant [5]. Different types of surface modification techniques have been used to increase osteointegration of the implants [142]. Alkali treatment (AT) is one of the surface modification techniques to enhance bioactivity of the implant [142]. AT at higher concentration forms a porous and bioactive surface layer on the implant [143]. Addition of heat treatment after AT produces porous network layers of sodium titanate [141] that enhance pull-out of the failure load and bone formation surrounding the implant [144]. Different temperatures and concentrations of NaOH or KOH were used to perform AT for several hours to modify the surface of the titanium [143]. Kim et al. [34] performed AT in 10 M NaOH or 10 M of KOH solution at 60 °C for 1-24 h. In another research study, AT

was performed in 10 M NaOH solution at 30°C for 24 h [35]. The AT was also conducted in lower concentration, i.e., 5M NaOH solution at 60 °C for 24 h [32].

The aim of this research was to optimize the AT to get web-like or nearly web-like structure. In this experiment, AT was carried out at three different concentrations of sodium hydroxide (NaOH), i.e., 5M, 10M and 15M. At each concentration, the experiment was performed at two different temperatures, 40 °C and 60 °C, with three different rotational speeds: 0, 30 and 60 rpm. To accomplish the aim, surface morphology was investigated by field emission scanning electron microscope (FESEM).

4.2 Materials and Methods

4.2.1 Materials

Commercially pure titanium (cp-Ti grade #2, President Titanium, MA, USA), ethanol (200 proof anhydrous), acetone (certified ACS), hydrofluoric acid (48-51% solution in water) and sodium hydroxide pellets (S318-1, Fisher Scientific).

4.2.2 Methods

Commercially pure titanium (Cp-Ti) samples with a diameter of 11 mm and thickness of 2 mm were used for AT. The samples were ground by using silicon carbide abrasive paper with a range of 320-800, followed by polishing using MasterTex polishing cloth. After polishing, samples were cleaned ultrasonically with DI water, ethanol, acetone and dried at atmospheric temperature. Then, AT was carried out at 5M, 10M and 15M concentrations of NaOH. At each concentration, the experiment was performed at 40 °C and 60 °C with three different rotational speeds: 0, 30 and 60 rpm for each temperature. The AT solution was prepared by dissolving NaOH in DI water.

Then, polished samples were immersed into the solution and incubated at predefined temperatures and rotational speeds for 24h. After 24h, samples were rinsed with DI water, ethanol and ultrasonically cleaned with DI water and finally dried at atmospheric temperature. The alkali heat-treated (AHT) samples were prepared by conducting heat treatment (HT) at 600 ℃ for 1h at a rate of 5 ℃/min after alkali treatment.

Material Characterization:

Surface morphology after AT was carried out by using field emission scanning electron microscope (FESEM, Hitachi model S4500).

***In Vitro* Cell Material Interaction:**

To understand the effects of surface modification of titanium by alkali experiment and heat treatment on proliferation of bone forming, human fetal osteoblast cells (hFOB 1.19, ATCC CRL-11372TM) were used. The culture medium used for osteoblast cells was a mixture of 1:1 Ham's F12 medium and Dulbecco's modified eagle's medium (DMEM) with 2.5 mM-glutamine (without phenol red; Sigma) supplemented by 10 % fetal bovine serum (FBS, ATCC), 1.2 g/L of NaHCO3 (Sigma), 0.3 mg/ml G 418 (Sigma) and penicillin/ streptomycin (Invitrogen, Germany) (10 mg/ml). Cells were cultured in 75 cm^3 vented cell culture flasks and maintained at 34 ℃ under an atmosphere of 5% CO2/ 95% air. Prior to cell culture, alkali-treated samples with following conditions were prepared: 5M at 60°C for 30 rpm and 10M at 60°C for 60 rpm. Then, polished titanium, alkali-treated titanium and AHT titanium were autoclaved to sterilize. A total of five different types of samples were used for the cell culture experiment: polished titanium, 5M-60°C-30 rpm alkali-treated titanium, 10M-60°C-60 rpm alkali-treated titanium, 5M-60°C-30rpm+HT

titanium and 10M-60°C-60rpm+HT titanium. Cells were seeded with a density of $2x10^5$ cells/substrate.

Cell Viability Assessment Using MTT Assay:

The MTT assay was performed after 2, 5 and 7 days of incubation to analyze the effect of web-like or nearly web-like structure formed by alkali experiment on osteoblast cells. The MTT (Life Technologies, Eugene, OR) solution of 0.5 mg/mL was prepared by dissolving MTT in sterile filtered PBS. One hundred microliters solution were added to each substrate in well plate, followed by 900 µL cell media addition and incubated at 34°C for osteoblast cells. After 2 h of incubation, the media was removed and 600 µL of solubilizer solution (composed of 10 % Triton X, 0.04 M HCl and isopropanol) were added to each substrate to dissolve formazan crystals. One hundred microliters solution were transferred to 96-well plate and read by UV visible spectrometer at a wavelength of 570 nm. Triplicate samples according to composition were evaluated and three measurements were performed from each substrate.

4.3 Results and Discussion

4.3.1 Results

Figure 18 shows the SEM micrograph of alkali-treated samples with a concentration of 5M NaOH solution at different temperatures and rotational speeds: (a) 40 °C, 30 rpm, (b) 60 °C, 0 rpm and (c) 60°C, 30 rpm. The experiment at each condition was performed repeatedly and nearly web-like structures were observed on the surface of the titanium.

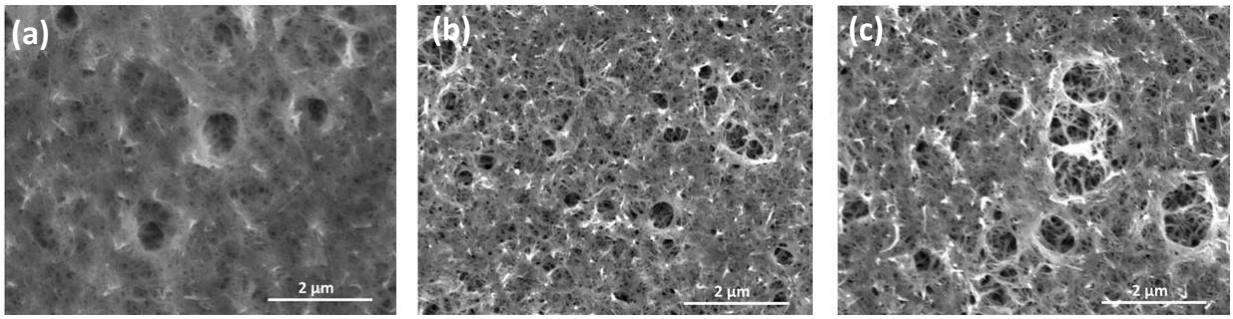

Figure 18: Surface morphology of alkali-treated samples with a concentration of 5M at different conditions: (a) 40 °C and 30 rpm (b) 60 °C and 0 rpm (c) 60 °C and 30 rpm.

The experiment was carried out at 5M NaOH solution with the following conditions: 40 °C, 0 rpm; 40 °C, 60 rpm; and 60 °C, 60 rpm, and the inconsistent surface morphology was found in the repeated experiment as a shown in Figure 19. Figure 19 (a-c) shows the surface morphology of the repeated experiment performed at 40 °C, 0 rpm and Figure 19 (d-f) shows the surface morphology of the experiment performed repeatedly at the same temperature but at 60 rpm. The same types of surface morphology were not observed in either condition for repeated experiments. The same trend was also observed when the experiments were performed repeatedly at 60 °C with a rotational speed of 60 rpm as shown in Figure 19 (g-i).

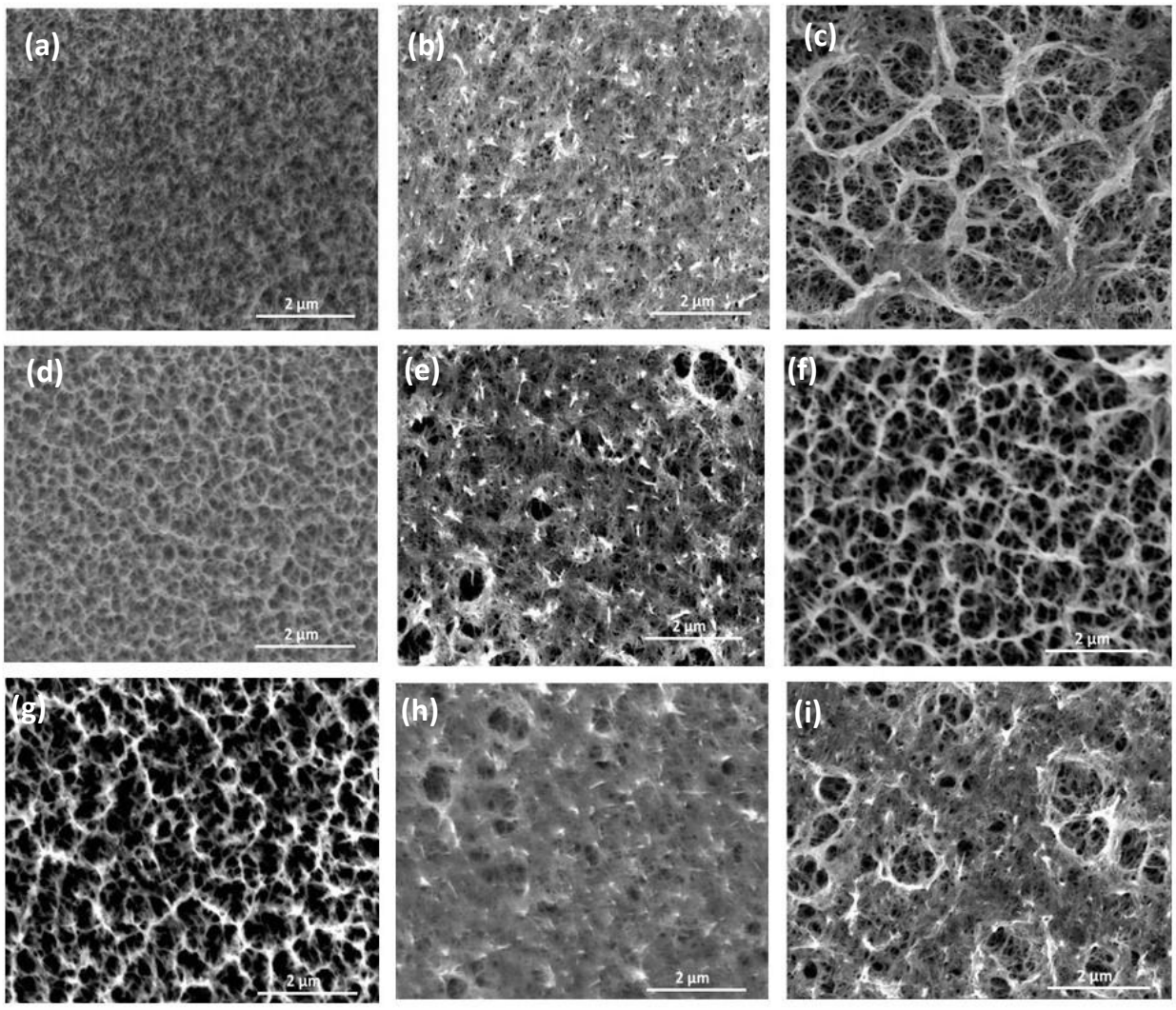

Figure 19: Surface morphology of alkali-treated samples at 5M NaOH solution with following conditions: (a-c) 40 °C, 0 rpm, (d-f) 40 °C, 60 rpm and (g-i) 60 °C, 60 rpm.

When the concentration of NaOH in alkali experiment was increased to 10 M, the web-like or porous-like structures formed on the surface in the following conditions: condition 1) 40 °C with the combination of three different rotational speeds of 0, 30 and 60 rpm; condition 2) 60°C with the combination of three different rotational speeds of 0, 30 and 60 rpm. Figure 20 shows the surface morphology of alkali-treated samples with a concentration of 10 M NaOH solution. Figure 20 (a-c) shows the surface morphology of porous or web-like network when the experiment was

carried out at 40°C for 24h with the rotational speed of 0, 30 and 60 rpm, respectively. Similarly, Figure 20 (d-f) shows the surface morphology of porous or web-like network when the experiment was carried out at 60°C for 24h with the rotational speed of 0, 30 and 60 rpm, respectively. In all combinations of experimental parameters, an identical porous network or web-like structure formed on the surface of the titanium samples.

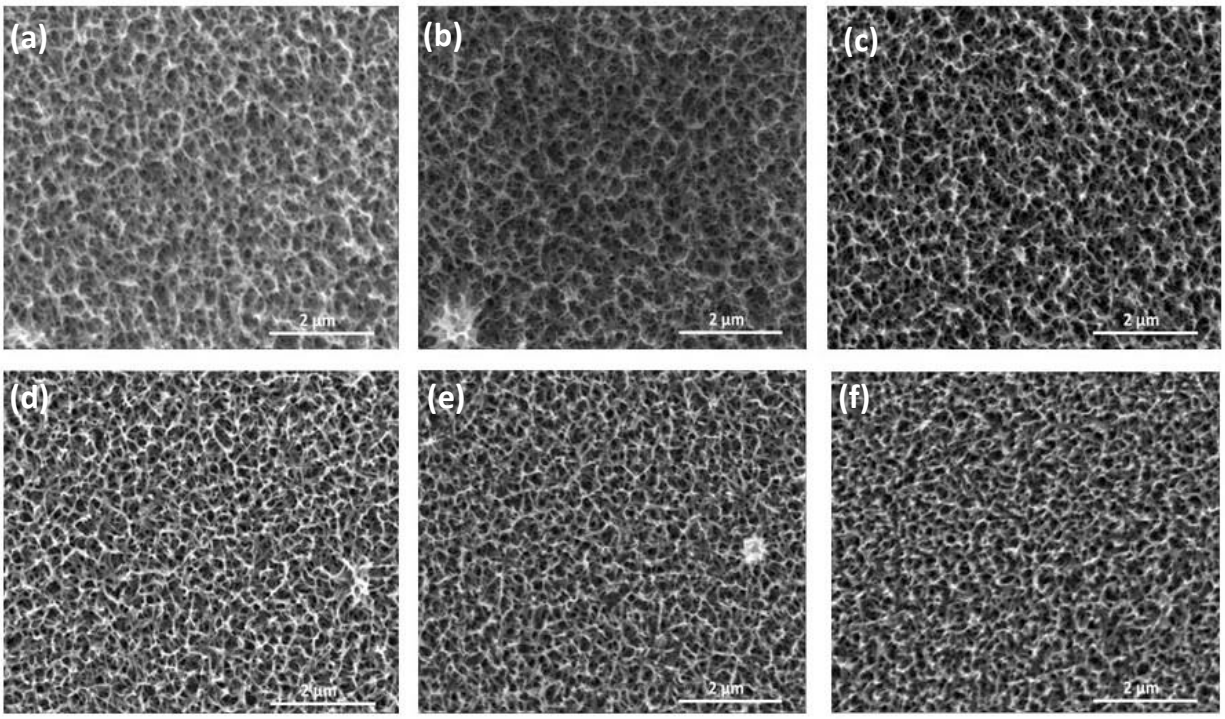

Figure 20: Surface morphology of alkali-treated samples with a concentration 10 M NaOH solutions at different combinations of temperatures and rotational speeds: (a) 40 °C, 0 rpm, (b) 40 °C, 30 rpm, (c) 40 °C, 60 rpm, (d) 60 °C, 0 rpm, (e) 60 °C, 30 rpm and (f) 60 °C, 60 rpm.

Figure 21 shows the surface morphology of alkali-treated samples; when the concentration of NaOH in AT experiment was increased to 15 M, cracks were formed in the porous or web-like structure in the following conditions: condition 1) 40 °C with the combination of three different rotation speeds of 0, 30 and 60 rpm; condition 2) 60°C with the combination of three different

rotation speeds of 0, 30 and 60 rpm. Figure 21 (a-c) shows the surface morphology of the alkali-treated samples when the experiment was carried out at 40°C with the rotational speeds of 0, 30 and 60 rpm, respectively. Similarly, cracks with web-like or porous structures were observed at 60°C with the rotational speeds of 0, 30 and 60 rpm, respectively, as shown in Figure 21 (d-f).

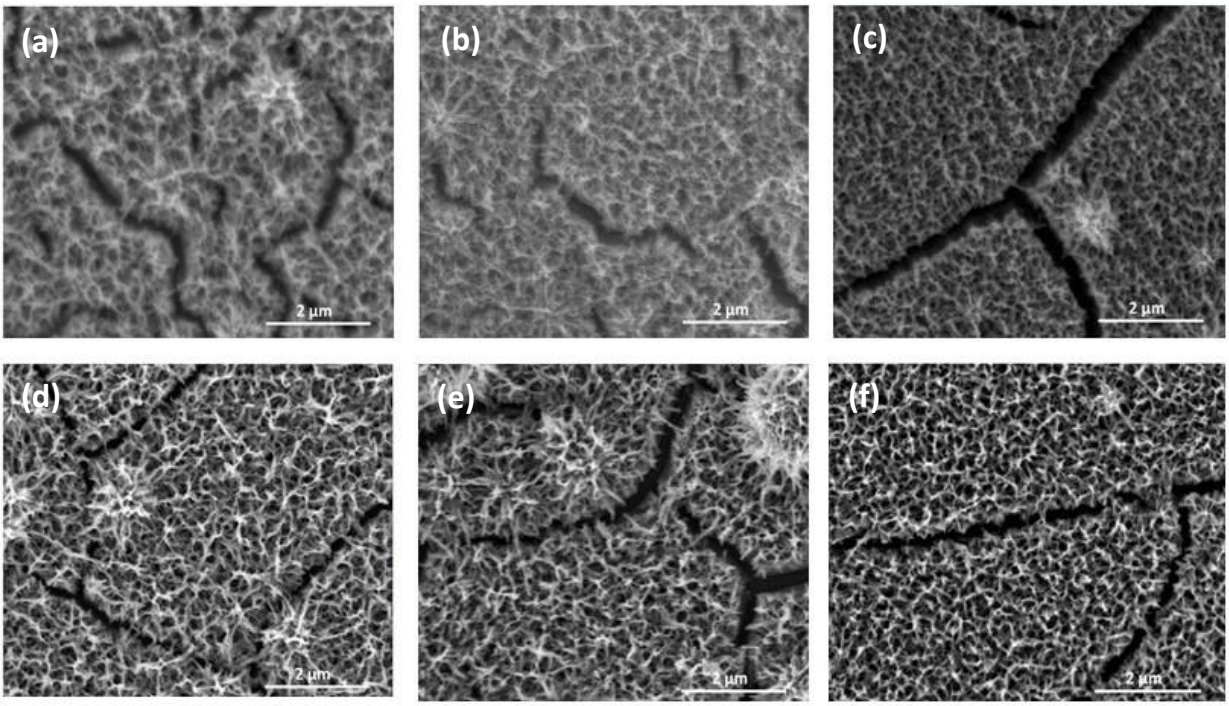

Figure 21: Surface morphology of alkali treated samples with a concentration 15 M NaOH solutions at different combinations of temperatures and rotational speeds: (a) 40 °C, 0 rpm, (b) 40 °C, 30 rpm, (c) 40 °C, 60 rpm, (d) 60 °C, 0 rpm, (e) 60 °C, 30 rpm and (f) 60 °C, 60 rpm.

Figure 22 shows the optical density of osteoblast cell proliferation after 2, 5 and 7 days of culture. After 2 days of culture, cell proliferation of polished titanium was higher compared to samples prepared by alkali-treated and AHT samples. The same trend was also observed after 5 and 7 days of culture. Among alkali treated and AHT, the sample prepared by AT with a concentration of 5 M at 60 °C for 30 rpm followed by heat treatment showed higher cell viability compared to other conditions of alkali-treated and AHT samples.

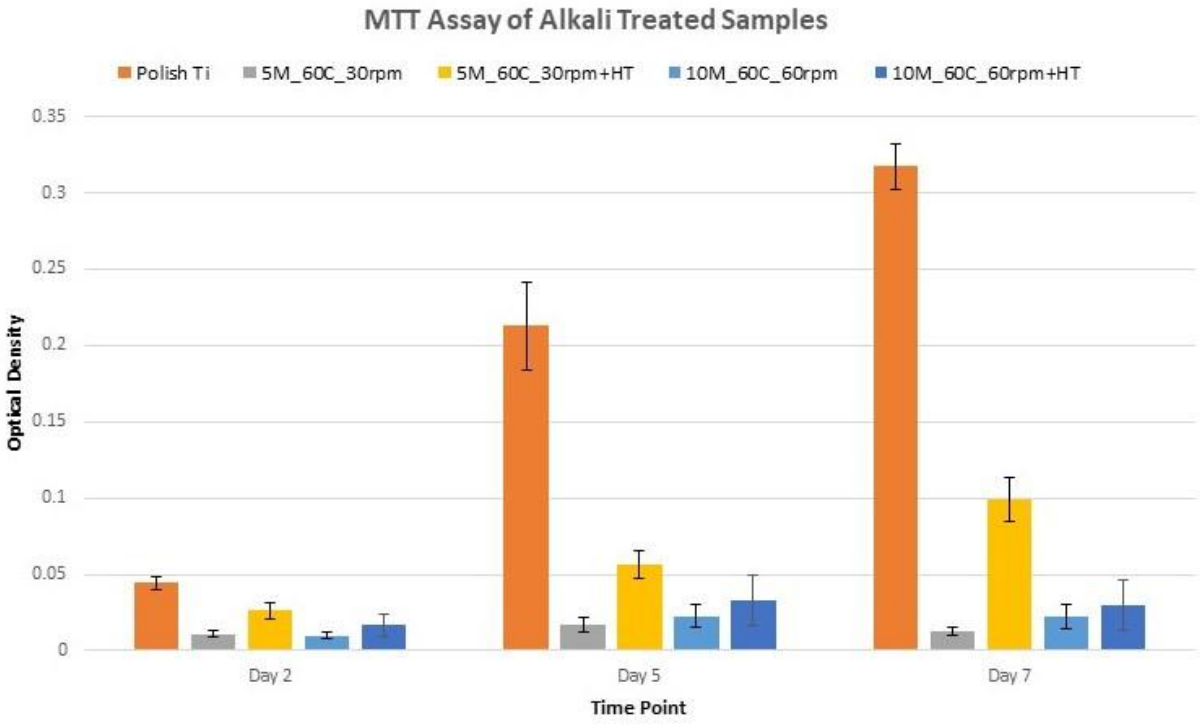

Figure 22: *In vitro* osteoblast cell viability of surface-modified titanium by alkali experiment at different temperatures and rotational speeds.

4.3.2 Discussion

The study investigates the effect of AT at different NaOH concentrations, temperatures and rotational speeds of samples on the formation of web-like or nearly web-like structure on the surface of pure titanium. When polished titanium samples are treated with NaOH solution during AT, a passive layer of TiO_2 on the surface partially dissolves in alkali solution due to the attack by hydroxyl groups which form $HTiO_3^-$ ions [34,142, 145]. This reaction is supposed to proceed simultaneously due to hydration of Ti as shown in following reactions [34,142]:

$$TiO_2 + NaOH \rightarrow HTiO_3^- + Na^+ \quad (1)$$

$$Ti + 3OH^- \rightarrow Ti(OH)_3^+ + 4e^- \quad (2)$$

$$Ti(OH)_3^+ + 4e^- \rightarrow TiO_2.H_2O + \frac{1}{2}H_2\uparrow \quad (3)$$

$$Ti(OH)_3^+ + OH^- \leftrightarrow Ti(OH)_4 \quad (4)$$

The hydrated TiO_2 layer is attacked by OH^- again and forms negatively charged hydrates on the surface of the samples [34,142,145]. These negatively charged hydrates combine with alkali ions in the aqueous solution, resulting in the formation of an alkali titanate hydrogel layer [34,142,145]:

$$TiO_2.H_2O + OH^- \leftrightarrow HTiO_3^-.\ nH_2O \quad (5)$$

Figure 18 shows nearly web-like structure formed at lower concentration of NaOH in AT solution. The reason for forming nearly web-like structure is due to the lower concentration of NaOH and immersion time, which allows less formation of sodium titanate on the surface [146]. The web-like structure formed on the surface is shown in Figure 20 when the concentration of NaOH increased to 10 M. The higher the molar concentration of NaOH causes more a noticeable titania layer, resulting in the formation of well-organized web-like structure on the surface [146]. In addition, the surface treatment in basic solution forms porous network structure due to the material erosion [147]. The material erosion depends on the concentration of eroding agent and immersion time in the solution [147]. If the concentration of eroding agent is high in the surface treatment solution, some of the irregularities and notches observed on the surface cause the potential crack initiation on the surface as shown in Figure 21 [147]. The crack formed at all

different combinations of temperatures and samples rotational speeds, which reveals no effects of temperature and sample rotation on surface morphology at 15M NaOH alkali-treated samples.

The formation of porous network structure depends on the corrosion of the surface. Corrosion resistance behavior of the surface of titanium also depends on the concentration and temperature at which the alkali experiment is carried out [148]. Corrosion resistance behavior deteriorates with the increase of concentration and temperature [148]. Figure 20 shows the images of alkali experiment carried out at 10 M NaOH with the increase of temperature and rotation speeds from 40°C-60°C and 0-60 rpm, respectively. Figure 20 (a-c) shows surface microstructure of the alkali experiment samples at 40 °C, which was less porous compared to the microstructure of the alkali experiment samples carried out at 60°C as shown in figure 20 (d-e). Thus, surface microstructures have significant effects on concentration of the NaOH in the solution and the temperature at which the experiment was performed.

The titanium plate treated with NaOH accelerates osteointegration [149]. The modified surface by NaOH treatment causes rapid protein adsorption and electrostatic attraction to the cells due to the hydrophilic nature of the modified surface [149]. A study was performed to investigate the biocompatibility of titanium nanostructure formed by alkali experiment or NaOH treatment where rat bone marrow (RBM) cells were used to analyze bioactivity [35]. The results showed that surface modified by alkali experiment and heat treatment enhanced cell adhesion and differentiation [35]. Figure 22 shows that polished titanium samples have higher cell viability compared to the titanium samples prepared by alkali experiments at different temperatures, rotational speeds, and heat treatment. The reason for this low viability was unexpected cell death. This unexpected cell death occurred due to a large volume cell media for cell seeding that caused

spilling of cell seeding media from the surface of the samples, resulting in the drying out of cell media during incubation. The surface formed by alkali experiment is more hydrophilic, and thus after seeding cells with media, the cell media spilled from the surface. Therefore, optimization is necessary to determine the exact way of cell seeding on the surface-modified titanium sample surface.

4.4 Conclusion

In this study, alkali treatment was carried out with different concentrations at different temperatures and rotational speeds of titanium sample to form web-like or nearly web-like structure and also to investigate the *in vitro* osteoblast cell viability. Alkali experiment was performed at three different concentrations of 5M, 10M and 15M NaOH at two different temperatures 40°C and 60°C. The experiment was carried out at three different rotational speeds of 0, 30 and 60 rpm, with the combination of each concentration and temperature. A nearly web-like or web-like structure formed at 5M and 10M concentrations while web-like structure with crack formed at a concentration of 15 M. The experiment with concentration of 5M at 40°C followed by 0 and 60 rpm and 60°C at 60 rpm did not obtain consistent morphology in repeated experiments. Based on the results, a nearly web-like structure formed by alkali experiment at 5M concentration of NaOH at 60°C and 30 rpm, and 10 M concentration of NaOH at 60°C and 60 rpm was used to investigate cell viability. Results showed that cell viability was less for surface-modified titanium compared to pure titanium because of cell seeding difficulties of rough surface. Optimization of cell culture is necessary to further investigate the cell viability of modified titanium samples.

CHAPTER 5 SUMMARY AND FUTURE DIRECTION

The purpose of this research was to understand the effect of ion incorporation into the surface-modified titanium, controlled release of aloe-emodin (AE) on surface-modified titatnium and its effect on *in vitro* cell interaction with surface modification by alkali experiment for orthopaedic applications. Some of the key conclusions of this research are:

1. Magnesium was incorporated into the modified titanium surface by different methods. Immersion methods, single-step anodization processes and reverse polarization techniques were used to dope magnesium into the modified titanium surface. In immersion methods with furnace drying followed by calcination, successful doping of magnesium with well-organized nanotubalar structures formed on the surface of the pure titanium. The magnesium content in nanotube structure decreased with the decreasing of magnesium nitrate concentration in solution. Single-step anodization was another method used for magnesium doping where two different anodization periods (45 mins and 70 mins) were used to perform the experiments. Magnesium was incorporated by anodization at 70 mins periods while only negligible amount of magnesium was doped at 45 mins time periods. At both time points, magnesium as well as residue due to chemical reaction formed on the surface, which covered some of the portion of nanotubal structures. The magnesium content in nanotubes decreased with the decreasing of magnesium nitrate concentration in electrolyte solutions. Other methods, named reverse polarization with different routes of drying, cleaning and

calcination processes, were used to incorporate magnesium into the surface-modified titanium. Magnesium-doped surface-modified titanium was found in this method. The magnesium content by reverse polarization was high, but nanotubal structures were slightly removed due to the reverse polarization process. Anodic oxidation was further carried out to investigate its effect on doping and nanotube formation. Results showed that less amount of magnesium doped and no well-organized nanotube structures formed. Thus, immersion method followed by drying and calcination was the most prominent methods to get magnesium-doped well-oganized nanotube structures.

2. Effect of controlled release of AE from surface-modified titanium and its *in vitro* interaction with osteoblast cells was invesitagated. Three different types of PLGA were used based on lactic acid (LA) and glycolic acid (GA) concentrations to observe the controlled AE release from titanium-modified surface. Results showed that addition of PLGA coating controlled the release of AE from modified titanium surface. After that, *in vitro* osteoblast cell culture study was performed on PLGA-coated (65:35) AE-loaded modified titanium samples for 2, 5, and 7 days time periods. Results showed that presence of AE enhanced osteoblast cell attachment and proliferation after 7 days of cultures for both PLGA- and No PLGA-coated samples. Therefore, the release of AE from develpoed implant increase osteoblast cell interaction and proliferation.
3. Alkali treatment was carried out with concentrations of 5M, 10M and 15M of NaOH at two different temperatures of 40°C and 60°C, repectively. The experiments with combination of each concentration and temperature were carried out at three different rotational speeds of sample incubation: 0, 30 and 60 rpm. The purpose of this study was to form web-like or nearly web-like structure. Results showed that nearly web-like

structure formed at 5M concentration of NaOH for the following combinations of temperature and rotational speeds: 40°C and 30 rpm, 60°C and 0 rpm, and 60°C and 30 rpm. Inconsistent results were found for all other combinations of temperature and rotation of speeds. The alkali experiment with 10 M concentrations at all combinations of temeprature and sample rotional speeds of incubation formed web-like structure on the surface. When the concentration was increased to 15 M, web-like structure with crack formed on the surface at all combinations of temperature and rotional speeds. Therefore, the alkali experiment at 10M concentration of NaOH showed uniform web-like structure in all combinations of temperature and rotation of speeds.

The data for the current research can be used to do further research on the following orthopedic and drug delivery applications:

1. *In vitro* cell culture study of Mg-doped modified titanium samples for bone formation.
2. Effect of controlled release of AE for cancer therapy in the implanted area.
3. Continuation of surface modification on titanium and different types of ion doping in titanium to investigate their effects in orthopedic applications.
4. To optimize and investigate the effect of *in vitro* osteoblast cell attachment and proliferation for alkali-treated samples with different combinations of NaOH at different temperatures and rotational speeds of incubated samples.

REFERENCES

[1] Qizhi Chen, George A. Thouas, “Metallic implant biomaterials”, Materials Science and Engineering R 87 (2015) 1–57.

[2] Takao Hanawa, “Biofunctionalization of Metallic Materials: Creation of Biosis–Abiosis Intelligent Interface”, Interface Oral Health Science 2014 pp 53-64.

[3] Emmanuel Gibon, Derek F. Amanatullah, Florence Loi, Jukka Pajarinen, Akira Nabeshima, Zhenyu Yao, Moussa Hamadouche, Stuart B. Goodman, “The Biological Response to Orthopaedic Implants for Joint Replacement: Part I: Metals”, J Biomed Mater Res B Appl Biomater. 2017 Oct;105(7):2162-2173.

[4] M Navarro, A Michiardi, O Castaño and J.A Planell, “Biomaterials in orthopaedics”, J. R. Soc. Interface 2008 5, 1137-1158.

[5] Virginia Sáenz de Viteri and Elena Fuentes, “Titanium and Titanium Alloys as Biomaterials”, Submitted: April 10th 2012Reviewed: January 15th 2013Published: May 22nd 2013.

[6] Buddy D. Ratner, Ph.D, Allan S. Hoffman, Sc.D, Frederick J. Schoen, M.D., Ph.D, Jack E. Lemons, Ph.D , “An Introduction to Materials in Medicine” Third Edition 2013.

[7] Kempland C. Walley BcS, Mergim Bajraliu BcS, Tyler Gonzalez MD, MBA, Ara Nazarian PhD, “The Chronicle of a Stainless Steel Orthopaedic Implant”, Volume 17 • June 2016.

[8] Takayuki Narushima, Kyosuke Ueda, Alfirano, “Co-Cr Alloys as Effective Metallic Biomaterials”, Advances in Metallic Biomaterials pp 157-178.

[9] T. Hryniewicz, R. Rokicki, K. Rokosz, “Co–Cr alloy corrosion behaviour after electropolishing and ‘magnetoelectropolishing’ treatments”, Materials Letters 62 (2008) 3073–3076.

[10] Kim EC, Kim MK, Leesungbok R, Lee SW, Ahn SJ, “Co-Cr dental alloys induces cytotoxicity and inflammatory responses via activation of Nrf2/antioxidant signaling pathways in human gingival fibroblasts and osteoblasts”, Dent Mater. 2016 Nov;32(11):1394-1405.

[11] M.İbrahim Coşkun, İsmail H.Karahan, YasinYücel, Teresa D.Golden, “Optimization of electrochemical step deposition for bioceramic hydroxyapatite coatings on CoCrMo implants”, Surface and Coatings Technology Volume 301, 15 September 2016, Pages 42-53.

[12] Youssef S. Al Jabbari, “Physico-mechanical properties and prosthodontic applications of Co-Cr dental alloys: a review of the literature”, J Adv Prosthodont 2014;6:138-45.

[13] Manmeet Kaur, K. Singh, “Review on titanium and titanium based alloys as biomaterials for orthopaedic applications”, Materials Science & Engineering C 102 (2019) 844–862.

[14] M. Niinomi and M. Nakai, “Titanium-Based Biomaterials for Preventing Stress Shielding between Implant Devices and Bone”, Hindawi Publishing Corporation, International Journal of Biomaterials, Volume 2011, Article ID 836587, 10 pages.

[15] Azhang Hamlekhan, Arman Butt, Sweetu Patel, Dmitry Royhman, Christos Takoudis, Cortino Sukotjo, Judy Yuan, Gregory Jursich, Mathew T. Mathew, William Hendrickson, Amarjit Virdi, Tolou Shokuhfar, “Fabrication of Anti-Aging TiO2 Nanotubes on Biomedical Ti Alloys”, PLOS ONE; May 2014 | Volume 9 | Issue 5 | e96213.

[16] Deval Prasad Bhattarai, Sita Shrestha, Bishnu Kumar Shrestha, Chan Hee Park, Cheol Sang Kim, “A controlled surface geometry of polyaniline doped titania nanotubes biointerface for accelerating MC3T3-E1 cells growth in bone tissue engineering”, Chemical Engineering Journal, Volume 350, 15 October 2018, Pages 57-68.

[17] Carlos Oldani and Alejandro Dominguez, “Titanium as a Biomaterial for Implants”, Submitted: February 17th 2011Reviewed: July 14th 2011Published: January 27th 2012, DOI: 10.5772/27413.

[18] Mukta Kulkarni, Anca Mazare, Patrik Schmuki, Aleš Iglič, “Biomaterial surface modification of titanium and titanium alloys for medical applications”, Nanomedicine, https://www.researchgate.net/publication/265292794.

[19] Sylwia Sobieszczyk, “Surface Modifications of Ti and its Alloys”, ADVANCES IN MATERIALS SCIENCE, Vol. 10, No. 1 (23), March 2010.

[20] Xuanyong Liu, Paul K. Chu, Chuanxian Ding, “Surface modification of titanium, titanium alloys, and related materials for biomedical applications”, Materials Science and Engineering R 47 (2004) 49–121.

[21] Anish Shivaram, Susmita Bose, Amit Bandyopadhyay, “Mechanical degradation of TiO2 nanotubes with and without nanoparticulate silver coating”, J Mech Behav Biomed Mater. 2016 Jun; 59:508-518.

[22] Yu Fu and Anchun Mo, “A Review on the Electrochemically Self organized Titania Nanotube Arrays: Synthesis, Modifications, and Biomedical Applications”, Fu and Mo Nanoscale Research Letters (2018) 13:187.

[23] D. Regonini, C.R. Bowen, A. Jaroenworaluck, R. Stevens, “A review of growth mechanism, structure and crystallinity of anodized TiO_2 nanotubes”, Materials Science and Engineering R 74 (2013) 377–406.

[24] Mustafa Erol, Tuncay Dikici, Mustafa Toparli, Erdal Celik, “The effect of anodization parameters on the formation of nanoporous TiO2 layers and their photocatalytic activities”, Journal of Alloys and Compounds 604 (2014) 66–72.

[25] Merve İzmir, Batur Ercan, “Anodization of titanium alloys for orthopedic applications”, Front. Chem. Sci. Eng., https://doi.org/10.1007/s11705-018-1759-y.

[26] Wang L N, Jin M, Zheng Y, Guan Y, Lu X, Luo J L, “Nanotubular surface modification of metallic implants via electrochemical anodization technique”, International Journal of Nanomedicine, 2014, 9(1): 4421–4435.

[27] Park J, Bauer S, von der Mark K, Schmuki P, “Nano size and vitality: TiO2 nanotube diameter directs cell fate”, Nano Lett. 7, 1686–1691 (2007).

[28] Sjöström T, Brydone AS, Meek RM, Dalby MJ, Su B, McNamara LE, “Titanium nano-featuring for enhanced bioactivity of implanted orthopedic and dental devices”, Nanomedicine (Lond). 2013 Jan;8(1):89-104. doi: 10.2217/nnm.12.177.

[29] Divya Rani VV, Vinoth-Kumar L, Anitha VC, Manzoor K, Deepthy M, Shantikumar VN, “Osteointegration of titanium implant is sensitive to specific nanostructure morphology”, Acta Biomater. 8, 1976–1989 (2012).

[30] Bjursten LM, Rasmusson L, Oh S, Smith GC, Brammer KS, Jin S, “Titanium dioxide nanotubes enhance bone bonding in vivo”, J. Biomed. Mater. Res. A. 92, 1218–1224 (2010).

[31] Karla S. Brammer, Seunghan Oh, Christine J. Cobb, Lars M. Bjursten, Henri van der Heyde, Sungho Jin, “Improved bone-forming functionality on diameter-controlled TiO_2 nanotube surface”, Acta Biomaterialia 5 (2009) 3215–3223.

[32] Shigeru Nishiguchi, Hirofumi Kato, Masashi Neo, Masanori Oka, Hyun-Min Kim, Tadashi Kokubo, Takashi Nakamura, “Alkali- and heat-treated porous titanium for orthopedic implants”, Journal of Biomedical Materials Research 54(2):198 – 208.

[33] V. Raman, S. Tamilselvi, N. Rajendran, “Electrochemical impedance spectroscopic characterization of titanium during alkali treatment and apatite growth in simulated body fluid”, Electrochimica Acta 52 (2007) 7418–7424.

[34] Hyun-Min Kim, Fumiaki Miyaji, Tadashi Kokubo, and Takashi Nakamura, “Preparation of bioactive Ti and its alloys via simple chemical surface treatment”, Journal of Biomedical Materials Research, Vol. 32, 409-417 (1996).

[35] Miho Fujio, Satoshi Komasa, Hiroshi Nishizaki, Tohru Sekino and Joji Okazaki, “Biocompatibility of titanium surface nanostructures following chemical processing and heat treatment”, Frontiers in Nanoscience and Nanotechnology.

[36] Sung-Pil Kim & Jong-Oh Kim, “Fabrication, characterization and photocatalytic performance of Fe-doped TiO2 nanotube composite for efficient degradation of water pollutants”, Desalination and Water Treatment.

[37] Ulf Helmersson, Martina Lattemann, Johan Bohlmark, Arutiun P. Ehiasarian, Jon Tomas Gudmundsson, “Ionized physical vapor deposition (IPVD): A review of technology and applications”, Thin Solid Films 513 (2006) 1–24.

[38] Ajay Vasudeo Rane, Krishnan Kanny, V.K. Abitha and Sabu Thomas, “Methods for Synthesis of Nanoparticles and Fabrication of Nanocomposites”, Synthesis of Inorganic Nanomaterials. https://doi.org/10.1016/B978-0-08-101975-7.00005-1.

[39] S.M. Rossnagel, “Directional and preferential sputtering-based physical vapor deposition”, Thin Solid Films 263 (1995) 1-12.

[40] S.Arul, M.Easwaramoorthi, M. meikandan, “Different Types Of PVD Coatings and their Demands – A Review”, International Journal of Applied Engineering Research ISSN 0973-4562 Volume 9, Number 24 (2014) pp. 26417-26430.

[41] Andresa Baptista, Francisco Silva, Jacobo Porteiro, José Míguez and Gustavo Pinto, “Sputtering Physical Vapour Deposition (PVD) Coatings: A Critical Review on Process Improvement and Market Trend Demands”, Coatings 2018, 8, 402; doi:10.3390/coatings8110402.

[42] Lingamaneni Prashanth, Kiran Kumar Kattapagari, Ravi Teja Chitturi, Venkat Ramana Reddy Baddam, Lingamaneni Krishna Prasad, “A review on role of essential trace elements in health and disease”, Journal of Dr. NTR University of Health Sciences 2015;4(2) 75-85.

[43] Fatih Karaaslan, Mahmut Mutlu, Musa Uğur Mermerkaya, Sinan Karaoğlu, Şerife Saçmaci, Şenol Kartal, “Comparison of bone tissue trace-element concentrations and mineral density in osteoporotic femoral neck fractures and osteoarthritis”, Clinical Interventions in Aging 2014:9 1375–1382.

[44] Ivana Zofková, Petra Nemcikova and Petr Matucha, “Trace elements and bone health”, Clin Chem Lab Med 2013; 51(8): 1555–1561.

[45] “Iron, Minerals and Trace Elements”, Journal of Pediatric Gastroenterology and Nutrition 41:S39–S46.

[46] Guifang Wang, Jinhua Li, [...], and Xinquan Jiang, “Magnesium ion implantation on a micro/nanostructured titanium surface promotes its bioactivity and osteogenic differentiation function”, International Journal of Nanomedicine 2014:9 2387–2398.

[47] Y. Yamasaki, Y. Yoshida, M. Okazaki, A. Shimazu, T. Uchida, T. Kubo, Y. Akagawa, Y. Hamada, J. Takahashi, N. Matsuura, “Synthesis of functionally graded MgCO3 apatite accelerating osteoblast adhesion”, J Biomed Mater Res. 2002 Oct;62(1):99-105.

[48] H. Zreiqat, C. R. Howlett, A. Zannettino, P. Evans, G. Schulze-Tanzil, C. Knabe, M. Shakibaei, “Mechanisms of magnesium-stimulated adhesion of osteoblastic cells to commonly used orthopaedic implants”, J Biomed Mater Res. 2002 Nov;62(2):175-84.

[49] Tetsuya Jinno, MD, PhD, Sarah K. Kirk, DVM, Sadao Morita, MD, PhD,† and Victor M. Goldberg, MD, “Effects of Calcium Ion Implantation on Osseointegration of Surface-Blasted Titanium Alloy Femoral Implants in a Canine Total Hip Arthroplasty Model”, The Journal of Arthroplasty Vol. 19 No. 1 2004.

[50] Edith Bonnelye, Anne Chabadel, Frédéric Saltel, Pierre Jurdic, “Dual effect of strontium ranelate: Stimulation of osteoblast differentiation and inhibition of osteoclast formation and resorption in vitro”, Bone 42 (2008) 129–138.

[51] Grynpas MD, Hamilton E, Cheung R, Tsouderos Y, Deloffre P, Hott M, Marie PJ, “Strontium increases vertebral bone volume in rats at a low dose that does not induce detectable mineralization defect”, Bone. 1996 Mar;18(3):253-9.

[52] A. Barbara, P. Delannoy, B.G. Denis, and P.J. Marie, “Normal Matrix Mineralization Induced by Strontium Ranelate in MC3T3-E1 Osteogenic Cells”, Metabolism, Vol 53, No 4 (April), 2004: pp 532-537.

[53] Hongjun Xie, Pei Wang & Jie Wu, “Effect of exposure of osteoblast-like cells to lowdose silver nanoparticles: uptake, retention and osteogenic activity”, Artificial Cells, Nanomedicine, and Biotechnology 2019, VOL. 47, NO. 1, 260–267.

[54] Sara Castiglioni, Alessandra Cazzaniga, Laura Locatelli and Jeanette A. M. Maier, “Silver Nanoparticles in Orthopedic Applications: New Insights on Their Effects on Osteogenic Cells”, Nanomaterials 2017, 7, 124; doi:10.3390/nano7060124.

[55] Brennan SA, Ní Fhoghlú C, Devitt BM, O'Mahony FJ, Brabazon D, Walsh A, “Silver nanoparticles and their orthopaedic applications”, Bone Joint J. 2015 May;97-B(5):582-9.

[56] Hua Geng, Gowsihan Poologasundarampillai, Naomi Todd, Aine Devlin-Mullin, Katie Moore, Zahra Golrokhi, James B. Gilchrist, Eric Jones, Richard J. Potter, Chris Sutcliffe, Marie O'Brien, David. W.L. Hukins, Sarah Cartmell, Christopher A. Mitchell, Peter D. Lee1, “Biotransformation of Silver Released from Nanoparticle Coated Titanium Implants Revealed in Regenerating Bone”, ACS Appl Mater Interfaces. 2017 Jun 28;9(25):21169-21180.

[57] Xinhua Qu, Zihao He, Han Qiao, Zanjing Zhai, Zhenyang Mao, Zhifeng Yu, Kerong Dai, “Serum copper levels are associated with bone mineral density and total fracture in the US population”, Journal of Orthopaedic Translation (2018) xx, 1-11.

[58] Giuseppe Della Pepa, Maria Luisa Brandi, “Microelements for bone boost: the last but not the least”, Clinical Cases in Mineral and Bone Metabolism 2016; 13(3):181-185.

[59] Gaurav Tiwari, Ruchi Tiwari, Birendra Sriwastawa, L Bhati, S Pandey, P Pandey, Saurabh K Bannerjee, “Drug delivery systems: An updated review”, International Journal of Pharmaceutical Investigation | January 2012 | Vol 2 | Issue 1.

[60] Kinam Park, “Drug Delivery Research: The Invention Cycle”, Mol. Pharmaceutics.

[61] D. Banerjee, S. Bose, “Comparative effects of controlled release of sodium bicarbonate and doxorubicin on osteoblast and osteosarcoma cell viability”, Materials Today Chemistry 12 (2019) 200e208.

[62] Yixiang Shi, Ajun Wan, Yifei Shi, Yueyue Zhang, and Yupeng Chen “Experimental and Mathematical Studies on the Drug Release Properties of Aspirin Loaded Chitosan Nanoparticles” Hindawi Publishing Corporation BioMed Research International, Volume 2014, Article ID 613619, 8 pages.

[63] Maher S, Mazinani A, Barati MR, Losic D, “Engineered titanium implants for localized drug delivery: recent advances and perspectives of Titania nanotubes arrays”, Expert Opin Drug Deliv. 2018 Oct;15(10):1021-1037.

[64] Qun Wang, Jian-Ying Huang, [...], and Yue-Kun Lai, “TiO2 nanotube platforms for smart drug delivery: a review”, Int J Nanomedicine. 2016; 11: 4819–4834.

[65] Jia H, Kerr LL, “Kinetics of drug release from drug carrier of polymer/TiO2 nanotubes composite-pH dependent study” J Appl Polym Sci. 2015;132:41750.

[66] Susmita Bose, Ashley Vu, Khalid Emshadi, Amit Bandyopadhyay, “Effects of polycaprolactone on alendronate drug release from Mgdoped hydroxyapatite coating on titanium”, Mater Sci Eng C Mater Biol Appl. 2018 Jul 1;88:166-171.

[67] M. Streckova, T. Sopcak, R. Stulajterova, M. Giretova, L. Medvecky, A. Kovalcikova, K. Balazsi, “Needle-less electrospinning employed for calcium and magnesium phosphate coatings on titanium substrates”, Surface and Coatings Technology, Volume 340, 25 April 2018, Pages 177-189.

[68] Jukka Lausmaa, “Surface spectroscopic characterization of titanium implant materials”, Journal of Electron Spectroscopy and Related Phenomena 81 (1996) 343-361.

[69] Xixue Hu, Hong Shen, Kegang Shuai, Enwei Zhang, Yanjie Bai, Yan Cheng, Xiaoling Xiong, Shenguo Wang, Jing Fang, Shicheng Wei, “Surface bioactivity modification of titanium by CO2 plasma treatment and induction of hydroxyapatite: In vitro and in vivo studies”, Applied Surface Science 257 (2011) 1813–1823.

[70] Ong JL, Carnes DL, Bessho K, “Evaluation of titanium plasma-sprayed and plasma-sprayed hydroxyapatite implants in vivo”, Biomaterials. 2004 Aug;25(19):4601-6.

[71] Vercaigne S, Wolke JG, Naert I, Jansen JA, “The effect of titanium plasma-sprayed implants on trabecular bone healing in the goat”, Biomaterials. 1998 Jun;19(11-12):1093-9.

[72] Yurong Yan, Yong Wei, Rui Yang, Lu Xia, Chenchen Zhao, Biao Gao, Xuming Zhang, Jijiang Fu, Qiong Wang, Na Xu, “Enhanced osteogenic differentiation of bone mesenchymal stem cells on magnesium-incorporated titania nanotube arrays” Colloids and Surfaces B: Biointerfaces 179 (2019) 309–316.

[73] Seung-Han Oh, Rita R. Fino˜ nes, Chiara Daraio, Li-Han Chen, Sungho Jin, “Growth of nano-scale hydroxyapatite using chemically treated titanium oxide nanotubes”, Biomaterials 26 (2005) 4938–4943.

[74] Lim HP, Park SW, Yun KD, Park C, Ji MK, Oh GJ, Lee JT, Lee K, “Hydroxyapatite Coating on TiO_2 Nanotube by Sol-Gel Method for Implant Applications”, J Nanosci Nanotechnol. 2018 Feb 1;18(2):1403-1405.

[75] Hans Gollwitzer, Maximilian Haenle, [...], and Norbert Harrasser, “A biocompatible sol–gel derived titania coating for medical implants with antibacterial modification by copper integration”, AMB Express. 2018; 8: 24.

[76] Shuilin Wu, Zhengyang Weng, Xiangmei Liu, K.W. K. Yeung, and Paul. K. Chu, “Functionalized TiO_2 Based Nanomaterials for Biomedical Applications”, Advanced Functional Materials Volume24, Issue35, September 17, 2014, Pages 5464-5481.

[77] Jiangdong Yu, Zhi Wu, Cheng Gong, Wang Xiao, Lan Sun and Changjian Lin, “Fe^{3+}-Doped TiO2 Nanotube Arrays on Ti-Fe Alloys for Enhanced Photo electrocatalytic Activity”, Nanomaterials 2016, 6, 107.

[78] Kunpeng Xie, Lan Sun, Chenglin Wang, Yuekun Lai, Mengye Wang, Hongbo Chen, Changjian Lin, “Photoelectrocatalytic properties of Ag nanoparticles loaded TiO2 nanotube arrays prepared by pulse current deposition”, Electrochimica Acta 55 (2010) 7211–7218.

[79] Awad NK, Edwards SL, Morsi YS, “A review of TiO2 NTs on Ti metal: Electrochemical synthesis, functionalization and potential use as bone implants”, Mater Sci Eng C Mater Biol Appl. 2017 Jul 1;76:1401-1412.

[80] Takashi Kizuki, Hiroaki Takadama, Tomiharu Matsushita, Takashi Nakamura, Tadashi Kokubo, “Preparation of bioactive Ti metal surface enriched with calcium ions by chemical treatment”, Acta Biomaterialia 6 (2010) 2836–2842.

[81] Verberckmoes SC, De Broe ME, D'Haese PC, “Dose-dependent effects of strontium on osteoblast function and mineralization”, Kidney Int. 2003 Aug;64(2):534-43.

[82] Karthika Prasad, Olha Bazaka, Ming Chua, Madison Rochford, Liam Fedrick, Jordan Spoor, Richard Symes, Marcus Tieppo, Cameron Collins, Alex Cao, David Markwell, Kostya (Ken) Ostrikov and Kateryna Bazaka, “Metallic Biomaterials: Current Challenges and Opportunities”, Materials 2017, 10, 884.

[83] Jiangdong Yu, Zhi Wu, Cheng Gong, Wang Xiao, Lan Sun and Changjian Lin, “Fe^{3+}-Doped TiO2 Nanotube Arrays on Ti-Fe Alloys for Enhanced Photoelectrocatalytic Activity”, Nanomaterials 2016, 6, 107.

[84] E.A. Al-Arfaj, “Structure and photocatalysis activity of silver doped titanium oxide nanotubes array for degradation of pollutants”, Superlattices and Microstructures 62 (2013) 285–291.

[85] Michael K. Seery, Reenamole George, Patrick Floris, Suresh C. Pillai, “Silver doped titanium dioxide nanomaterials for enhanced visible light photocatalysis”, Journal of Photochemistry and Photobiology A: Chemistry 189 (2007) 258–263.

[86] Ika Maria Ulfah, Boy M. Bachtiar, Arnita Rut Murnandityas and Slamet, “Synthesis and Characterization of Ag-Doped TiO2 Nanotubes on Ti-6Al-4V and Ti-6Al-7Nb Alloy”, Proceedings of the International Seminar on Metallurgy and Materials (ISMM2017).

[87] Qi Wu, Junjie Ouyang, Kunpeng Xie, Lan Sun, Mengye Wang, Changjian Lin, “Ultrasound-assisted synthesis and visible-light-driven photocatalytic activity of Fe-incorporated TiO2 nanotube array photocatalysts”, Journal of Hazardous Materials 199– 200 (2012) 410– 417.

[88] Sofia A. Alves, Sweetu B. Patel, Cortino Sukotjo, Mathew T. Mathew, Paulo N. Filho, Jean-Pierre Celis, Luís A. Rocha, Tolou Shokuhfar, “Synthesis of calcium-phosphorous doped TiO2 nanotubes by anodization and reverse polarization: A promising strategy for an efficient biofunctional implant surface”, Applied Surface Science 399 (2017) 682–701.

[89] Yiqiang Yu, Guodong Jin, Yang Xue, Donghui Wang, Xuanyong Liu, Jiao Sun, “Multifunctions of dual Zn/Mg ion co-implanted titanium on osteogenesis, angiogenesis and bacteria inhibition for dental implants”, Acta Biomater. 2017 Feb;49:590-603.

[90] Yajing Yan, Qiongqiong Ding, Yong Huang, Shuguang Han, Xiaofeng Pang, “Magnesium substituted hydroxyapatite coating on titanium withnanotublar TiO2intermediate layer via electrochemical deposition”, Applied Surface Science 305 (2014) 77–85.

[91] Murali Krishna Duvvuru, Weiguo Han, Prantik Roy Chowdhury, Sahar Vahabzadeh, Federico Sciammarella, Sherine F. Elsawa, “Bone marrow stromal cells interaction with titanium; Effects of composition and surface modification”, PLOS ONE | https://doi.org/10.1371/journal.pone.0216087 May 22, 2019.

[92] Rabiatul Basria S.M.N. Mydin, Roshasnorlyza Hazan, Mustafa Fadzil FaridWajidi and Srimala Sreekantan, “Titanium Dioxide Nanotube Arrays for Biomedical Implant Materials and Nanomedicine Applications”, IntechOpen, http://dx.doi.org/10.5772/intechopen.73060.

[93] E. P. Su, D. F. Justin, C. R. Pratt, V. K. Sarin, V. S. Nguyen, S. Oh, S. Jin, “Effects of titanium nanotubes on the osseointegration, cell differentiation, mineralisation and antibacterial properties of orthopaedic implant surfaces”, Bone Joint J. 2018 Jan; 100-B(1 Supple A): 9–16.

[94] Sofia A. Alves, Sweetu B. Patel, Cortino Sukotjo, Mathew T. Mathew, Paulo N. Filho, Jean-Pierre Celis, Luís A. Rocha, Tolou Shokuhfar, “Synthesis of calcium-phosphorous doped TiO2 nanotubes by anodization and reverse polarization: A promising strategy for an efficient biofunctional implant surface”, Applied Surface Science 399 (2017) 682–701.

[95] Sofia A.Alves, André L.Rossi, Ana R.Ribeiro, Jacques Werckmann, Jean-Pierre Celis, Luís A.Rocha,Tolou Shokuhfar, “A first insight on the bio-functionalization mechanisms of TiO2 nanotubes with calcium, phosphorous and zinc by reverse polarization anodization, Surface and Coatings Technology”, Volume 324, 15 September 2017, Pages 153-166.

[96] Sabina Grigorescu, Vasile Pruna, Irina Titorencu, Victor V. Jinga, Anca Mazare, Patrik Schmuki, Ioana Demetrescu, “The two step nanotube formation on TiZr as scaffolds for cell growth”, Bioelectrochemistry 98 (2014) 39–45.

[97] Gopal K. Mor, Oomman K. Varghese, Maggie Paulose, Karthik Shankar, Craig A. Grimes, “A review on highly ordered, vertically oriented TiO2 nanotube arrays: Fabrication, material properties, and solar energy applications”, Solar Energy Materials & Solar Cells 90 (2006) 2011–2075.

[98] L. Sun, J.Li, C.L.Wang, S.F.Li, H.B.Chen, C.J.Lin, “An electrochemical strategy of doping Fe3+ intoTiO2 nanotube array films for Enhancement in photocatalytic activity”, Solar Energy Materials & Solar Cells 93(2009)1875–1880.

[99] R. Torresi, O. Camara, C. De Pauli, “Influence of the hydrogen evolution reaction on the anodic titanium oxide film properties”, Electrochimica Acta 32(1987) 1357–1363.

[100] Naboneeta Sarkar, and Susmita Bose, “Controlled delivery of curcumin and vitamin K2 from HA-coated Ti implant for enhanced in vitro chemoprevention, osteogenesis and in vivo osseointegration”, ACS Appl. Mater. Interfaces 2020, XXXX, XXX, XXX-XXX.

[101] E. K. Hefni, S. Bencharit, S. J. Kim, K. M. Byrd, T. Moreli, F. H. Nociti, S. Offenbacher and S. P. Barros, “Transcriptomic profiling of tantalum metal implant osseointegration in osteopenic patients”, BDJ Open (2018) 4:17042.

[102] Francesco Roberto Evola, Maria Elena Cucuzza, Giuseppe Evola, “Osteosarcoma in the pediatric age”, EUROMEDITERRANEAN BIOMEDICAL JOURNAL 2018,13 (29) 127-131.

[103] Amirhossein Misaghi, Amanda Goldin, Moayd Awad, and Anna A Kulidjian, “Osteosarcoma: a comprehensive review”, SICOT-J 2018, 4, 12.

[104] Franchi Marco, Fini Milena, Giavaresi Gianluca, Ottani Vittoria, “Peri-implant osteogenesis in health and osteoporosis” , Micron 36 (2005) 630–644.

[105] Liu Y, Rath B, Tingart M, Eschweiler J, “Role of implants surface modification in osseointegration: A systematic review”, J Biomed Mater Res A. 2020 Mar;108(3):470-484.

[106] Amir Zareidoost, Mardali Yousefpour, Behrooz Ghaseme, Amir Amanzadeh, “The relationship of surface roughness and cell response of chemical surface modification of titanium”, J Mater Sci: Mater Med (2012) 23:1479–1488.

[107] Qi Liu, Wenjun Li, Liang Cao, Jiajia Wang, Yingmin Qu, Xinyue Wang, Rongxian Qiu, Xu Di, Zuobin Wang, Bojian Liang, “Response of MG63 Osteoblast Cells to Surface Modification of Ti-6Al-4V Implant Alloy by Laser Interference Lithography”, Journal of Bionic Engineering 14 (2017) 448–458.

[108] Xiaohui Rausch-fan, Zhe Qu, Marco Wieland, Michael Matejka, Andreas Schedle, “Differentiation and cytokine synthesis of human alveolar osteoblasts compared to osteoblast-like cells (MG63) in response to titanium surfaces”, dental materials 2 4 (2 0 0 8) 102–110.

[109] Abel Santos, Moom Sinn Aw, Manpreet Bariana, Tushar Kumeria, Ye Wang and Dusan Losic, “Drug-releasing implants: current progress, challenges and perspectives”, J. Mater. Chem. B, 2014, 2, 6157–6182.

[110] Sarah A. Stewart, Juan Domínguez-Robles, Ryan F. Donnelly and Eneko Larrañeta, “Implantable Polymeric Drug Delivery Devices: Classification, Manufacture, Materials, and Clinical Applications”, Polymers 2018, 10, 1379.

[111] Ashleigh Anderson, James Davis, “Design of functionalized materials for use in micro nanoscale drug delivery devices and smart patches”, Nanostructures for Drug Delivery”, Micro and Nano Technologies 2017, Pages 183-206.

[112] Himanshu Agrawal, Nipa Thacker, Ambikanandan Misra, “Parenteral Delivery of Peptides and Proteins”, Challenges in Delivery of Therapeutic Genomics and Proteomics 2011, Pages 531-622.

[113] Xuetao Shi, Yingjun Wang, Li Ren, Wei Huang, Dong-An Wang, “A protein/antibiotic releasing poly(lactic-co-glycolic acid)/lecithin scaffold for bone repair applications”, International Journal of Pharmaceutics 373 (2009) 85–92.

[114] Krishna Suri, Joy Wolfram, Haifa Shen, Mauro Ferrari, “Advances in Nanotechnology-Based Drug Delivery Platforms and Novel Drug Delivery Systems”, Novel Approaches and Strategies for Biologics, Vaccines and Cancer Therapies 2015, Pages 41-58.

[115] Anoop Kumar, JonathanPillai, “Implantable drug delivery systems: An overview”, Nanostructures for the Engineering of Cells, Tissues and Organs 2018, Pages 473-511.

[116] Neda Alasvand, Aleksandra M. Urbanska, Maryam Rahmati, Maryam Saeidifar, P. Selcan Gungor-Ozkerim, Farshid Sefat, Jayakumar Rajadas and Masoud Mozafari, “Therapeutic

Nanoparticles for Targeted Delivery of Anticancer Drugs", Multifunctional Systems for Combined Delivery, Biosensing and Diagnostics. http://dx.doi.org/10.1016/B978-0-323-52725-5.00013-7.

[117] Pooja R. Alli, Pratima B. Bargaje, Nilesh S. Mhaske, "Sustained Release Drug Delivery System: A Modern Formulation Approach", Asian Journal of Pharmaceutical Technology & Innovation, 04 (17); 2016; 108 – 118.

[118] Y. Raghunathan, L. Amsel, O. Hinsvark, W. Bryant, "Sustained-release drug delivery system I: Coated ion-exchange resin system for phenylpropanolamine and other drugs", Journal of Pharmaceutical Sciences Vol. 70, No. 4, April 1981.

[119] Jessica A. Lyndon, Ben J. Boyd, Nick Birbilis, "Metallic implant drug/device combinations for controlled drug release in orthopaedic applications", Journal of Controlled Release xxx (2014) xxx–xxx.

[120] Alicja Kazek-Kęsik, Agnieszka Nosol, Joanna Płonka, Monika Śmiga-Matuszowicz Monika Gołda-Cępa, Małgorzata Krok-Borkowicz, Monika Brzychczy-Włoch, Elżbieta Pamuła, Wojciech Simka, "PLGA-amoxicillin-loaded layer formed on anodized Ti alloy as a hybrid material for dental implant applications", Materials Science & Engineering C 94 (2019) 998–1008.

[121] Cortizo MC, Oberti TG, Cortizo MS, Cortizo AM, Fernández Lorenzo de Mele MA, "Chlorhexidine delivery system from titanium/polybenzyl acrylate coating: Evaluation of cytotoxicity and early bacterial adhesion", Journal of dentistry 40 (2012) 329-337.

[122] Kashi TS, Eskandarion S, Esfandyari-Manesh M, Marashi SM, Samadi N, Fatemi SM, Atyabi F, Eshraghi S, Dinarvand R, "Improved drug loading and antibacterial activity of minocycline-loaded PLGA nanoparticles prepared by solid/oil/water ion pairing method", Int J Nanomedicine. 2012;7:221-34.

[123] Piergiorgio Gentile, Valeria Chiono, [...], and Paul V. Hatton, "An Overview of Poly(lactic-co-glycolic) Acid (PLGA)-Based Biomaterials for Bone Tissue Engineering", Int. J. Mol. Sci. 2014, 15, 3640-3659.

[124] Teresa Pecere, M. Vittoria Gazzola, Carla Mucignat, Cristina Parolin, Francesca Dalla Vecchia, Andrea Cavaggioni, Giuseppe Basso, Alberto Diaspro, Benedetto Salvato, Modesto Carli, and Giorgio Palu` [2], "Aloe-emodin Is a New Type of Anticancer Agent with Selective Activity against Neuroectodermal Tumors", CANCER RESEARCH 60, 2800–2804, June 1, 2000.

[125] Josias H. Hamman, "Composition and Applications of Aloe vera Leaf Gel", *Molecules* 2008, 13, 1599-1616.

[126] Pandurangan Subash-Babu and Ali A. Alshatwi, "Aloe-Emodin inhibits adipocyte differentiation and maturation during in vitro Human Mesenchymal Stem cell adipogenesis", J Biochem Molecular Toxicology Volume 00, Number 0, 2012.

[127] S.K. Agarwal, Sudhir S. Singh, Sushma Verma, Sushil Kumar, "Antifungal activity of anthraquinone derivatives from *Rheum emodi*", Journal of Ethnopharmacology 72 (2000) 43–46.

[128] Park MY, Kwon HJ, Sung MK, "Evaluation of aloin and aloe-emodin as anti-inflammatory agents in aloe by using murine macrophages", Biosci Biotechnol Biochem. 2009 Apr 23;73(4):828-32.

[129] Su-Ui Lee, Hye Kyoung Shin, Yong Ki Min, Seong Hwan Kim, “Emodin accelerates osteoblast differentiation through phosphatidylinositol 3-kinase activation and bone morphogenetic protein-2 gene expression”, International Immunopharmacology (2008) 8, 741—747.

[130] Yutthana Pengjam, Harishkumar Madhyastha, Radha Madhyastha, Yuya Yamaguchi, Yuichi Nakajima and Masugi Maruyama, “Anthraquinone Glycoside Aloin Induces Osteogenic Initiation of MC3T3-E1 Cells: Involvement of MAPK Mediated Wnt and Bmp Signaling”, Biomol Ther 24(2), 123-131 (2016).

[131] Dishary Banerjee and Susmita Bose, “Effects of Aloe Vera Gel Extract in Doped Hydroxyapatite-Coated Titanium Implants on in Vivo and in Vitro Biological Properties”, ACS Appl. Bio Mater. XXXX, XXX, XXX−XXX.

[132] Solaiman Tarafder, Kelly Nansen, Susmita Bose, “Lovastatin release from polycaprolactone coated β-tricalcium phosphate: Effects of pH, concentration and drug–polymer interactions”, Materials Science and Engineering C 33 (2013) 3121–3128.

[133] Pinghua Tu, Qiu Huang, Yunsheng Ou, Xing Du, Kaiting Li, Yong Tao and Hang Yin, “Aloe-emodin-mediated photodynamic therapy induces autophagy and apoptosis in human osteosarcoma cell line MG-63 through the ROS/JNK signaling pathway”, ONCOLOGY REPORTS 35: 3209-3215, 2016.

[134] Mahesh Sapkota, Saroj Kumar Shrestha, Ming Yang, Young Ran Park, Yunjo Soh, “Aloe-emodin inhibits osteogenic differentiation and calcification of mouse vascular smooth muscle cells”, European Journal of Pharmacology xxx (xxxx) xxxx.

[135] Y. Yang, N. Oh, Y. Liu, W. Chen, S. Oh, M. Appleford, S. Kim, K. Kim, S. Park, J. Bumgardner, W. Haggard, and J. Ong, “Enhancing Osseointegration Using Surface-Modified Titanium Implants”, JOM 58, 71–76 (2006). https://doi.org/10.1007/s11837-006-0146-1.

[136] Larsson C, Thomsen P, Aronsson BO, Rodahl M, Lausmaa J, Kasemo B, Ericson LE, “Bone response to surface-modified titanium implants: studies on the early tissue response to machined and electropolished implants with different oxide thicknesses”, Biomaterials. 1996 Mar;17(6):605-16.

[137] Solaiman Tarafder and Susmita Bose, “Polycaprolactone-Coated 3D Printed Tricalcium Phosphate Scaffolds for Bone Tissue Engineering: In Vitro Alendronate Release Behavior and Local Delivery Effect on In Vivo Osteogenesis”, ACS Applied Materials & Interfaces; dx.doi.org/10.1021/am501048n | ACS Appl. Mater. Interfaces 2014, 6, 9955−9965.

[138] Bose S, Vu AA, Emshadi K, Bandyopadhyay A, “Effects of polycaprolactone on alendronate drug release from Mg-doped hydroxyapatite coating on titanium”, Mater Sci Eng C Mater Biol Appl. 2018 Jul 1;88:166-171.

[139] Soares IMV, Fernandes GVO, Larissa Cordeiro C, Leite YKPC, Bezerra DO, Carvalho MAM, Carvalho CMRS, “The influence of Aloe vera with mesenchymal stem cells from dental pulp on bone regeneration: characterization and treatment of non-critical defects of the tibia in rats”, J Appl Oral Sci. 2019;27:e20180103.

[140] Wang RR, Fenton A, “Titanium for prosthodontic applications: a review of the literature”, Quintessence Int 1996;27:401-8.

[141] Baek-Hee Lee, Young Do Kim, Ji Hoon Shin, Kyu Hwan Lee, “Surface modification by alkali and heat treatments in titanium alloys”, J Biomed Mater Res. 2002 Sep 5;61(3):466-73.

[142] Y. Sasikumar K. Indira · N. Rajendran, “Surface Modification Methods for Titanium and Its Alloys and Their Corrosion Behavior in Biological Environment: A Review”, Journal of Bio- and Tribo-Corrosion (2019) 5:36, DOI: 10.1007/s40735-019-0229-5.

[143] By Lai-Chang Zhang, Liang-Yu Chen, and Liqiang Wang, “Surface modification of titanium and titanium alloys: technologies, developments and future interests”, Advanced Engineering Materials, https://doi.org/10.1002/adem.201901258.

[144] Shigeru Nishiguchi, Shunsuke Fujibayashi, Hyun-Min Kim, Tadashi Kokubo, Takashi Nakamura, “Biology of alkali- and heat-treated titanium implants”, J Biomed Mater Res A. 2003 Oct 1;67(1):26-35.

[145] Xuefeng Hu, Koon Gee Neoh, Jieyu Zhang, En-Tang Kang, “Bacterial and osteoblast behavior on titanium, cobalt–chromium alloy and stainless steel treated with alkali and heat: A comparative study for potential orthopedic applications”, Journal of Colloid and Interface Science 417 (2014) 410–419.

[146] Suzan Bsat, Saber Amin Yavari, Maximilian Munsch, Edward R. Valstar and Amir A. Zadpoor, “Effect of Alkali-Acid-Heat Chemical Surface Treatment on Electron Beam Melted Porous Titanium and Its Apatite Forming Ability”, Materials 2015, 8, 1612-1625.

[147] Amin Yavari S, Ahmadi SM, van der Stok J, Wauthle R, Riemslag AC, Janssen M, Schrooten J, Weinans H, Zadpoor AA, “Effects of bio-functionalizing surface treatments on the mechanical behavior of open porous titanium biomaterials”, J Mech Behav Biomed Mater. 2014 Aug;36: 109-19.

[148] A. A. Al-asnawy, A. A. El-hadad, Islam S. EL-Sayed, Khairy M. T. Eraba, “Thermochemical Modification of Ti–6Al–4V alloy for Biomedical Applications”, 2016 IJSRSET | Volume 2 | Issue 5 | Print ISSN: 2395-1990 | Online ISSN: 2394-4099.

[149] Miryam Cuellar-Flores, Laura Susana Acosta-Torres, Omar Martínez-Alvarez, Benjamin Sánchez-Trocino, Javier de la Fuente-Hernández, Rigoberto Garcia-Garduño, and Rene Garcia-Contreras, “Effects of alkaline treatment for fibroblastic adhesion on titanium”, Dent Res J (Isfahan). 2016 Nov-Dec; 13(6): 473–477.